Nilpotent center in continuous piecewise quadratic polynomial Hamiltonian vector fields

Ting Chen
School of Statistics and Mathematics, Guangdong University of Finance and Economics, Guangzhou, 510320, P.R. China,
chenting0715@126.com

Jaume Llibre
Departament de Matemàtiques, Universitat Autònoma de Barcelona, 08193 Bellaterra, Barcelona, Spain
jllibre@mat.uab.cat

In this paper we study the global dynamics of continuous piecewise quadratic Hamiltonian systems separated by the straight line $x = 0$, where these kinds of systems have a nilpotent center at $(0, 0)$, which comes from the combination of two cusps of both Hamiltonian systems. By the Poincaré compactification we classify the global phase portraits of these systems. We must mention that it is extremely rare to find works studying the center-focus problem in piecewise smooth systems with non-elementary singular points as we did here.

Keywords: Nilpotent, Bi-center, Hamiltonian, Phase portrait.

1. Introduction and statement of the main results

From the works of Poincaré [Poincaré, 1881] and Dulac [Dulac, 1908] the center-focus problem, i.e the problem of distinguishing when a singular point is either a focus or a center, has been one of main problems in the qualitative theory of the planar differential equations. In the planar polynomial vector fields a singular point is either elementary or non-elementary. The linear part of the elementary singular point has at least one nonzero eigenvalue, and the non-elementary one has two zero eigenvalues. And a non-elementary singular point is called nilpotent if its linear part is not identically zero, otherwise is called degenerate. Moreover, if a planar polynomial differential equation has a *linear type center*, a *nilpotent center* and a *degenerate center* at the origin, after affine change of time and variables, this differential equation can be written as

$$(\dot{x}, \dot{y}) = \left\{ \begin{array}{l} (-y,\ x) \\ (y,\ 0) \\ (0,\ 0) \end{array} \right\} + (F(x, y), G(x, y)), \tag{1}$$

respectively, where $F(x, y)$ and $G(x, y)$ are real polynomials without constant and linear terms.

The center-focus problem in the quadratic polynomial differential equations has been solved see [Artés & Llibre, 1994; Bautin, 1952; Kapteyn, 1911, 1912; Schlomiuk, 1993; Żołądek, 1994]. For the cubic polyno-

mial differential equations there are partial works in the center-focus problem, see [Aziz, Llibre & Pantazi, 2014; Cima & Llibre, 1990; Malkin, 1964; Vulpe & Sibirskii, 1988; Żołądek, 1994, 1996] for an update of these works. Recently, Colak *el at.* [Colak *et al.*, 2014] studied the phase portraits of some cubic Hamiltonian differential equations with a linear type center at the origin. The authors of [Chen *et al.*, 2020] investigated the Z_2-equivariant linear type bi-center problem for cubic polynomial Hamiltonian systems.

It is well known that the center-focus problem for non-elementary singular points becomes more difficult. Computationally efficient methods have been developed to find the center conditions for planar systems with nilpotent singular points, see [Garcia *et al.*, 2016; Liu & Li, 2015, 2011; Stróżzyna *et al.*, 2012]. Note that quadratic polynomial equations do not have nilpotent centers, i.e. the simplest nilpotent centers must appear in cubic differential equations [Nusse & Yorke , 1995]. The phase portraits of some cubic Hamiltonian vector fields with a nilpotent center at the origin were classified in [Colak *et al.*, 2014]. Li *el at.* [Li *et al.*, 2018] study the bi-center conditions for a class of Z_2-equivariant cubic differential equations with two nilpotent singular points.

In recent years an increasing interest appears for studying the qualitative theory of the non-smooth differential equations, mainly due to the fact that these equations can analyze some real phenomena more accurately, see for instance [Andronov *et al.*, 1966; Banerjee & Verghese, 2001; Filippov, 1988; Lv *et al.*, 2019].

In this paper we will study the following piecewise smooth systems,

$$(\dot{x},\dot{y}) = \left(F^{\pm}(x,y), G^{\pm}(x,y)\right), \qquad \pm s(x,y) \geq 0, \tag{2}$$

where $(F^{+}(x,y), G^{+}(x,y))$ and $(F^{-}(x,y), G^{-}(x,y))$ are smooth vector fields, and they are separated by the discontinuity curve $\Gamma = s^{-1}(0)$.

The center-focus problem in the piecewise smooth systems becomes much more complicated than that in the smooth systems. Gasull and Torregrosa [Gasull & Torregrosa, 2003] developed an efficient method for computing the Lyapunov constants of piecewise smooth systems (2), which can be used to solve the center-focus problem of piecewise smooth systems with linear type singular points. By computing the Lyapunov constants, the authors of [Chen & Zhang, 2012; Tian *et al.*, 2015] gave a complete classification on the linear type center conditions of the origin in several classes of Bautin switching systems. There are some results for determining the linear type center conditions in cubic piecewise smooth systems, see [Coll *et al.*, 1999; Guo *et al.*, 2019].

As far as we known there is extremely rare to find works for studying the center-focus problem in piecewise smooth systems with non-elementary singular points, see [Chen *et al.*, 2021, 2018]. This work is more challenging compared to the smooth systems.

In this paper using the Poincaré compactification we will study the global dynamics of a class of piecewise quadratic Hamiltonian systems with a nilpotent type center at $(0,0)$ which comes from the combination of two cusps of both Hamiltonian systems, described by

$$\begin{pmatrix}\dot{x}\\ \dot{y}\end{pmatrix} = \begin{cases} \begin{pmatrix} y + a_{20}x^2 - 2b_{02}xy + a_{02}y^2 \\ -x^2 - 2a_{20}xy + b_{02}y^2 \end{pmatrix}, & \text{for } \ x \geq 0, \\ \begin{pmatrix} y + A_{20}x^2 - 2b_{02}xy + a_{02}y^2 \\ x^2 - 2A_{20}xy + b_{02}y^2 \end{pmatrix}, & \text{for } \ x \leq 0, \end{cases} \tag{3}$$

where $x = 0$ is the discontinuity line, a_{20}, a_{02}, b_{02} and A_{20} are real parameters. Note that systems (3) are continuous on $x = 0$. The Hamiltonian functions of the right system and the left one of systems (3) are

$$H(x,y)^{+} = \frac{1}{3}x^3 + \frac{1}{2}y^2 + a_{20}x^2y - b_{02}xy^2 + \frac{a_{02}}{3}y^3 \tag{4}$$

and

$$H(x,y)^{-} = -\frac{1}{3}x^3 + \frac{1}{2}y^2 + A_{20}x^2y - b_{02}xy^2 + \frac{a_{02}}{3}y^3, \tag{5}$$

respectively.

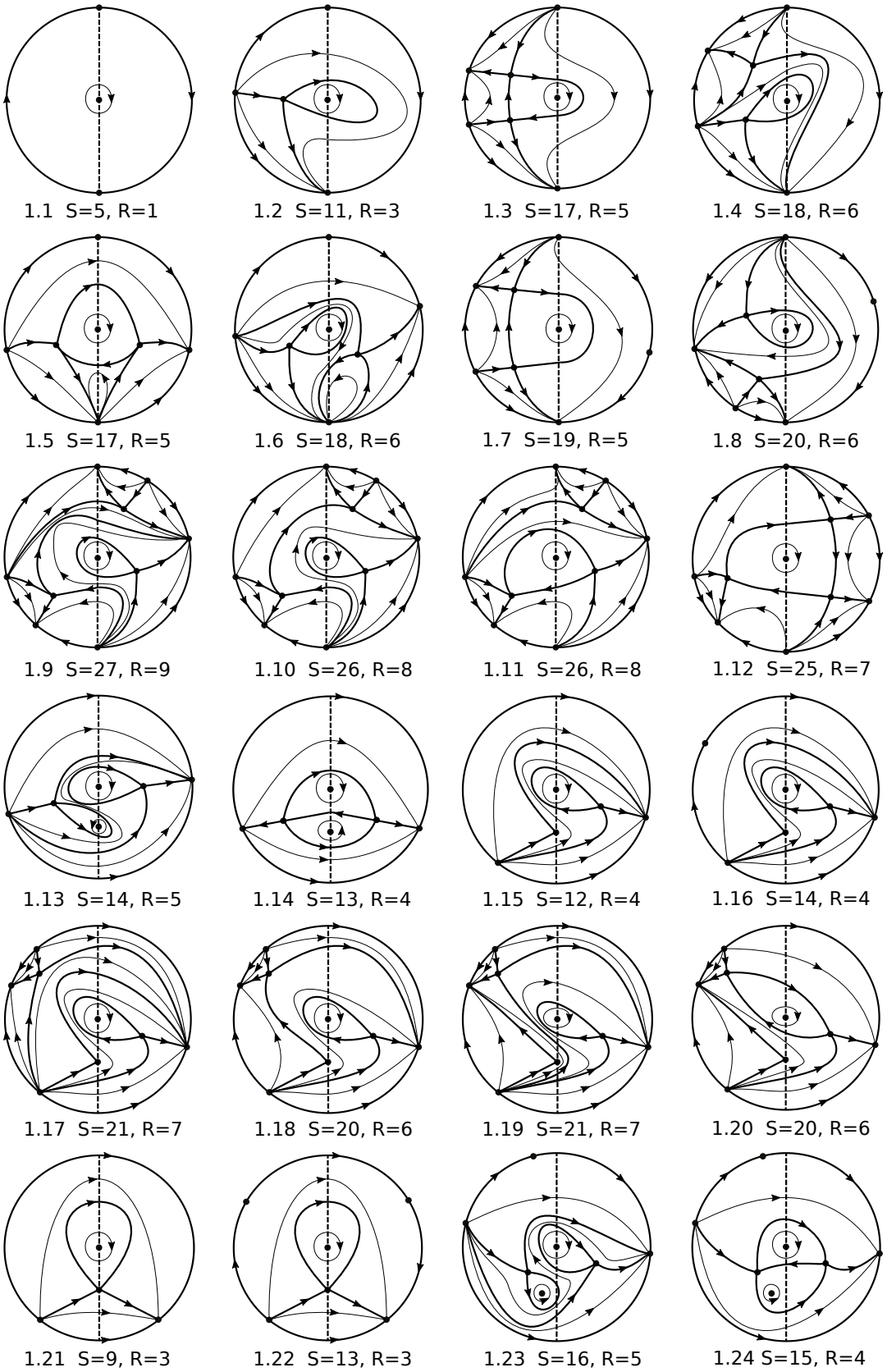

Fig. 1. Topological phase portraits of cases 1.1-1.24 of Proposition 1.

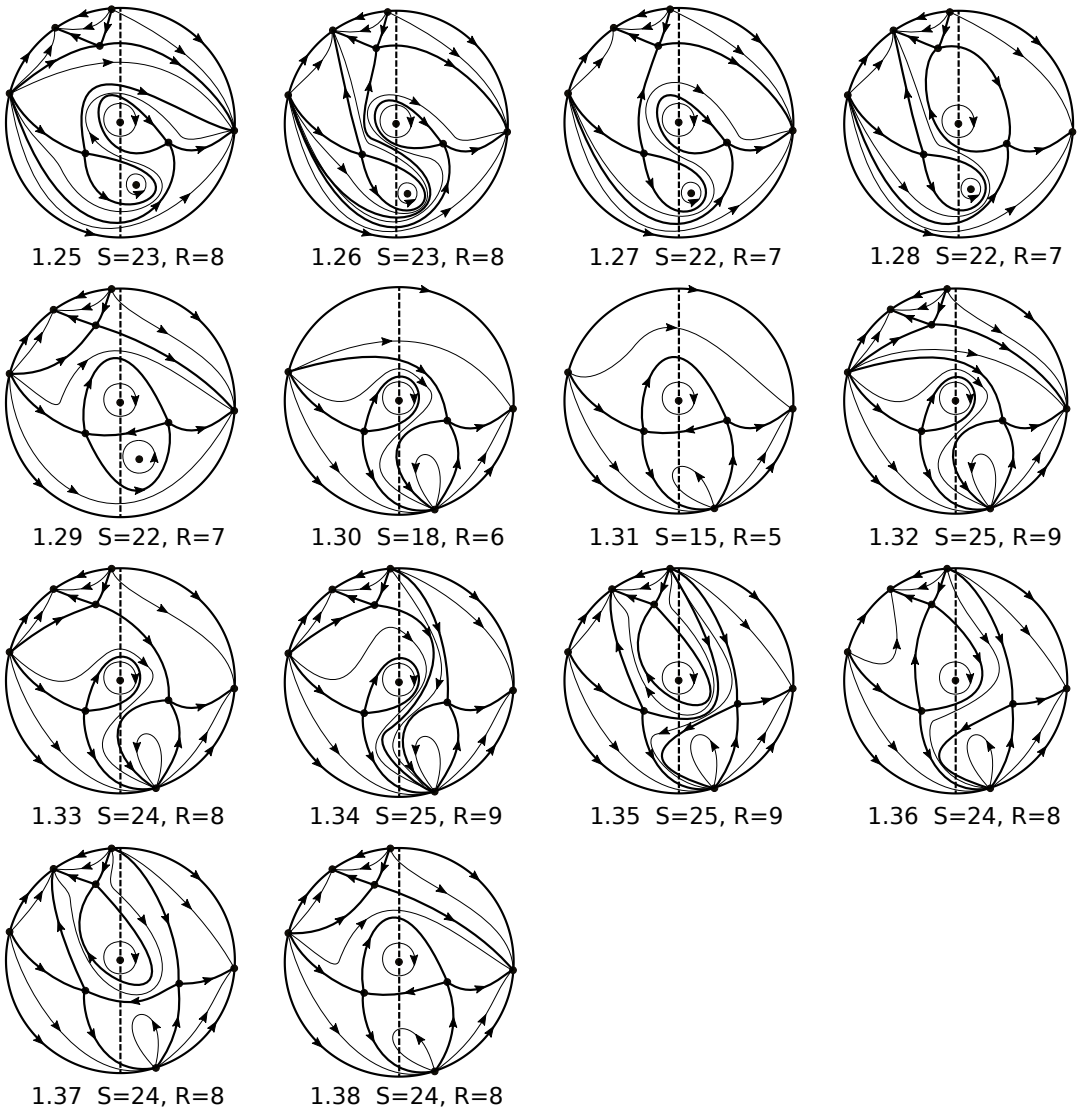

Fig. 2. Topological phase portraits of cases 1.25-1.38 of Proposition 1.

We denote by S and R the number of *separatrices* and of *canonical regions* of a phase portrait in the Poincaré disc $\mathbb{D}^2$, respectively. It is known that a separatrix of a polynomial differential system in the Poincaré disc is an orbit such that the orbits in one side of this orbit have different α- or ω-limit than the orbits in the other side of this orbit in any small neighborhood of it. And the separatrices include all the infinite orbits, all the finite singular points, the two orbits at the boundary of the hyperbolic sectors of the finite and infinite singular points, the limit cycles. If Σ denotes the closed set of all separatrices in the Poincaré disc $\mathbb{D}^2$, and the components of $\mathbb{D}^2 \setminus \Sigma$ are called the canonical regions. For more details on separatrices and canonical regions see Chapter 1 of [Dumortier *et al.*, 2006].

Our main result is the following one.

Theorem 1. *In the Poincaré disc the phase portraits of systems* (3) *with a nilpotent center at* $(0,0)$ *are topologically equivalent to the following* 38 *phase portraits of Figures 1 and 2.*

In Section 2 we provide a brief introduction to the Poincaré compactification and some basic results that we shall need for proving Proposition 1. In Section 3 we show how to obtain the continuous piecewise quadratic Hamiltonian systems (3). In Section 4 we characterize the global phase portraits of systems (3) in the Poincaré disc.

2. Preliminaries

2.1. *Poincaré compactification*

In order to study the phase portrait of the infinite singular points of systems (3) we use the Poincaré compactification, see more details in Chapter 5 of [Dumortier *et al.*, 2006]. In fact this compactification identifies the plane $\mathbb{R}^2$ with the interior of the closed unit disc $\mathbb{D}^2$ centered at the origin of coordinates of the plane, and extends analytically the differential systems to its boundary, usually called the circle of the infinity. The singular points in the interior of the disc $\mathbb{D}^2$ are called *finite singular points*, and the ones on the boundary of $\mathbb{D}^2$ are called *infinite singular points*.

In the planar $\mathbb{R}^2$ we describe the Poincaré compactification for the piecewise polynomial differential systems

$$(\dot{x_1}, \dot{x_2}) = \left(X^{\pm}(x_1, x_2), Y^{\pm}(x_1, x_2)\right), \qquad \pm x_1 \geq 0, \tag{6}$$

whose associated polynomial vector fields are $P^+ = (X^+(x_1, x_2), Y^+(x_1, x_2))$ and $P^- = (X^-(x_1, x_2), Y^-(x_1, x_2))$, respectively. The degree of P^+ is the maximum of the degrees of the polynomials X^+ and Y^+, in a similar way is defined the degree of P^-. The degrees of P^+ and P^- are defined as d^+ and d^-, respectively.

For studying the neighborhood of the boundary of the disc $\mathbb{D}^2$, i.e the neighborhood of the infinity of $\mathbb{R}^2$, we use four local charts $U_i = \{(x_1, x_2) \in \mathbb{D}^2 : x_i > 0\}$ and $V_i = \{(x_1, x_2) \in \mathbb{D}^2 : x_i < 0\}$, for $i = 1, 2$, with the corresponding diffeomorphisms

$$\phi_i : \ U_i \to \mathbb{R}^2, \qquad \psi_i : \ V_i \to \mathbb{R}^2, \tag{7}$$

defined by $\phi_i(x_1, x_2) = (x_2/x_1, 1/x_1) = (u, v)$ and $\psi_i(x_1, x_2) = (x_1/x_2, 1/x_2) = (u, v)$. Thus the coordinates (u, v) play different roles in the distinct local charts. The expressions for the corresponding vector fields (6) in the local charts U_1 and V_1 are given by

$$(\dot{u}, \dot{v}) = \left(v^{d^+}\left[-uX^+\left(\frac{1}{v}, \frac{u}{v}\right) + Y^+\left(\frac{1}{v}, \frac{u}{v}\right)\right], -v^{d^+ + 1}X^+\left(\frac{1}{v}, \frac{u}{v}\right)\right) \tag{8}$$

and

$$(\dot{u}, \dot{v}) = \left((-1)^{d^- - 1}v^{d^-}\left[-uX^-\left(\frac{1}{v}, \frac{u}{v}\right) + Y^-\left(\frac{1}{v}, \frac{u}{v}\right)\right], (-1)^{d^-}v^{d^- + 1}X^-\left(\frac{1}{v}, \frac{u}{v}\right)\right) \tag{9}$$

respectively. And the expressions of vector fields (6) in the local chart U_2 with $u \geq 0$ and $u \leq 0$ are given by

$$(\dot{u}, \dot{v}) = \left(v^{d^+}\left[X^+\left(\frac{u}{v}, \frac{1}{v}\right) - uY^+\left(\frac{u}{v}, \frac{1}{v}\right)\right], -v^{d^+ + 1}Y^+\left(\frac{u}{v}, \frac{1}{v}\right)\right), \tag{10}$$

and

$$(\dot{u}, \dot{v}) = \left(v^{d^-}\left[X^-\left(\frac{u}{v}, \frac{1}{v}\right) - uY^-\left(\frac{u}{v}, \frac{1}{v}\right)\right], -v^{d^- + 1}Y^-\left(\frac{u}{v}, \frac{1}{v}\right)\right), \tag{11}$$

respectively. The expressions of the vector fields (6) in the local chart V_2 with $u \geq 0$ and $u \leq 0$ are equal to the expressions in the local chart U_2 multiplied by $(-1)^{d^+ - 1}$ and $(-1)^{d^- - 1}$, respectively. In fact it is sufficient to study the infinite singular points in $U_1|_{v=0}$ and $V_1|_{v=0}$, and at the origin of U_2 and V_2 for studying all the infinite singular points of systems (6). Note that when the origin of U_2 is an infinite singular point it comes from the combination of the two origins of systems (10) and (11).

2.2. *Topological skeleton*

The union of the set of all separatrices with an orbit of each canonical region form the *separatix skeleton*. We say that the separatrix skeletons S_1 and S_2 of the flows $(\mathbb{D}^2, \phi_1)$ and $(\mathbb{D}^2, \phi_2)$ are *topologically equivalent* if there exists a homeomorphism $h : S_1 \to S_2$ which sends orbits to orbits reversing or preserving the direction of all orbits. In a similar way it is defined the topological equivalence between the flows $(\mathbb{D}^2, \phi_1)$

and $(\mathbb{D}^2, \phi_2)$. From [Markus, 1954; Neumann, 1975; Peixoto, 1973] we have the following theorem which is enough to describe the separatrix skeleton in order to determine the topological equivalence class of a differential system in the Poincaré disc $\mathbb{D}^2$.

Theorem 2 [Markus–Neumann–Peixoto Theorem]. *Assume that $(\mathbb{D}^2, \phi_1)$ and $(\mathbb{D}^2, \phi_2)$ are two continuous flows with only isolated singular points. Then these flows are topologically equivalent if and only if their separatrix skeletons are topological equivalent.*

2.3. *Topological index*

Then we present two important theorems on the topological index of a singular point in differential systems on surfaces, which are extremely useful tools to analyze the type of the singular points, for more details see Chapter 6 of [Dumortier *et al.*, 2006].

Theorem 3. *We denote by p an isolated singular point with the finite sectorial decomposition property. Let q, h and e be the number of parabolic, hyperbolic and elliptic sectors of p, respectively. Then the topological index of the singular point p equals $1 + (e - h)/2$.*

Corollary 2.1. *The topological indices of a center, a cusp, a saddle and a node equal 1, 0, -1 and 1, respectively.*

Theorem 4. *For any continuous vector field with finitely many singular points, the sum of their topological indices is 2.*

3. Obtaining systems (3)

Without loss of generality the piecewise quadratic Hamiltonian systems (3) are obtained from the more general quadratic differential systems having a nilpotent singular point at the origin of coordinates, i.e.

$$\begin{pmatrix} \dot{x} \\ \dot{y} \end{pmatrix} = \begin{cases} \begin{pmatrix} y + a_{20}x^2 + a_{11}xy + a_{02}y^2 = F^+(x,y) \\ b_{20}x^2 + b_{11}xy + b_{02}y^2 = G^+(x,y) \end{pmatrix}, & \text{for } x \geq 0, \\ \begin{pmatrix} y + A_{20}x^2 + A_{11}xy + A_{02}y^2 = F^-(x,y) \\ B_{20}x^2 + B_{11}xy + B_{02}y^2 = G^-(x,y) \end{pmatrix}, & \text{for } x \leq 0. \end{cases} \tag{12}$$

Let $H^+(x,y)$ be the cubic Hamiltonian of the right system of systems (12). Integrating $G^+(x,y)$ of (12) with respect to x and we have

$$\begin{aligned} H_1^+(x,y) =& h_1(y) - \int G^+(x,y)dx \\ =& h_1(y) - \frac{b_{20}}{3}x^3 - \frac{b_{11}}{2}x^2y - b_{02}xy^2, \end{aligned} \tag{13}$$

for some real polynomials h_1. And integrating $F^+(x,y)$ of (12) with respect to y and we have

$$\begin{aligned} H_2^+(x,y) =& h_2(x) + \int F^+(x,y)dy \\ =& h_2(x) + \frac{1}{2}y^2 + a_{20}x^2y + \frac{a_{11}}{2}xy^2 + \frac{a_{02}}{3}y^3, \end{aligned} \tag{14}$$

for some real polynomials h_2. We equate $H_1^+(x,y)$ to $H_2^+(x,y)$ and have

$$a_{11} = -2b_{02}, \qquad b_{11} = -2a_{20}, \tag{15}$$

$h_1(y) = y^2/2 + a_{02}y^3/3$ and $h_2(x) = -b_{20}x^3/3$. Similar to the right system of (12), we have

$$A_{11} = -2B_{02}, \qquad B_{11} = -2A_{20}, \tag{16}$$

from the left one of (12).

Then systems (12) become the piecewise quadratic Hamiltonian systems

$$\begin{pmatrix}\dot{x}\\ \dot{y}\end{pmatrix} = \begin{cases} \begin{pmatrix} y + a_{20}x^2 - 2b_{02}xy + a_{02}y^2 = y + \Phi^+(x,y) \\ b_{20}x^2 - 2a_{20}xy + b_{02}y^2 = \Psi^+(x,y)\end{pmatrix}, & \text{for } x \geq 0, \\ \begin{pmatrix} y + A_{20}x^2 - 2B_{02}xy + A_{02}y^2 = y + \Phi^-(x,y) \\ B_{20}x^2 - 2A_{20}xy + B_{02}y^2 = \Psi^-(x,y)\end{pmatrix}, & \text{for } x \leq 0. \end{cases} \tag{17}$$

For analyzing the origin of the right and the left systems of (17), we define

$$f^{\pm}(x) = \sum_{k=2}^{\infty} c_k^{\pm} x^k$$

as the unique solution of $y + \Phi^{\pm}(x,y) = 0$ in a neighborhood of the origin, respectively. And assuming that

$$\Psi^{\pm}(x, f^{\pm}(x)) = \sum_{k=2}^{\infty} \alpha_k^{\pm} x^k. \tag{18}$$

It follows from Theorem 3.5 of [Dumortier *et al.*, 2006] that when $\alpha_m \neq 0$ and

$$\begin{cases} m = 2k+1 & \begin{cases} \alpha_m < 0, \textit{ then the origin is a center or a focus}, \\ \alpha_m > 0, \textit{ then the origin is a saddle}, \end{cases} \\ m = 2k, \textit{ then the origin is a cusp}. \end{cases} \tag{19}$$

We note that a_{20} and A_{20} cannot be zero, otherwise the positive y-axis or the negative one are invariant and consequently the origin of the piecewise differential systems cannot be center. From the above results we have the following for the right system and the left one of the piecewise Hamiltonian systems (17):

$$\begin{aligned} \alpha_2^+ &= b_{20}, \quad \alpha_3^+ = 2a_{20}^2, \\ \alpha_2^- &= B_{20}, \quad \alpha_3^- = 2A_{20}^2. \end{aligned} \tag{20}$$

In short, if $\alpha_2^{\pm} \neq 0$ then the corresponding Hamiltonian system of the continuous piecewise differential systems (17) has a cusp at the origin. But if $\alpha_2^{\pm} = 0$, since $\alpha_3^{\pm} > 0$, then the corresponding Hamiltonian system has a saddle, and then the continuous piecewise differential systems (17) cannot have a center at the origin. So we must assume that $\alpha_2^{\pm} \neq 0$.

In summary, the piecewise differential systems (17) only can have a center at the origin if both Hamiltonian systems have a cusp at the origin. Therefore, assume that $b_{20} \neq 0$ and $B_{20} \neq 0$ and consequently $\alpha_2^+ \neq 0$ and $\alpha_2^- \neq 0$.

If we have a periodic orbit around the origin of the piecewise differential systems (17) which intersects the straight line $x = 0$ in the points $(0, y_1)$ and $(0, y_2)$ with $y_1 < y_2$ and both different from zero, then y_1 and y_2 must be solutions of $H^+(0,y_1) - H^+(0,y_2) = (y_1 - y_2)e_1/6 = 0$ and $H^-(0,y_1) - H^-(0,y_2) = (y_1 - y_2)e_2/6 = 0$, where

$$\begin{aligned} e_1 &= 3y_1 + 2a_{02}y_1^2 + 3y_2 + 2a_{02}y_1y_2 + 2a_{02}y_2^2, \\ e_2 &= 3y_1 + 2A_{02}y_1^2 + 3y_2 + 2A_{02}y_1y_2 + 2A_{02}y_2^2. \end{aligned}$$

We calculate the Gröbner basis for the two polynomials e_1 and e_2, and obtain three polynomials $(a_{02} - A_{02})y_2^2$, $(a_{02} - A_{02})(y_1 + y_2)$ and $3y_1 + 2A_{02}y_1^2 + 3y_2 + 2A_{02}y_1y_2 + 2A_{02}y_2^2$. Note that if $A_{02} = a_{02}$ then we have a continuum of solutions for y_1 and y_2, and consequently we can have a continuum of periodic orbits, which allow the existence of centers surrounding the origin. Therefore in what follows $A_{02} = a_{02}$.

Note that if $A_{02} \neq a_{02}$, then $y_2 = 0$ and we cannot have periodic orbits, because they cannot pass through the singular point of the piecewise differential system localized at the origin of coordinates.

In order that the piecewise differential systems (17) be continuous on $x = 0$, i.e., $\Psi^+(x,y)|_{x=0} = \Psi^-(x,y)|_{x=0}$ we obtain $B_{02} = b_{02}$. Otherwise there will be more complex bifurcations. Hence with the two conditions $A_{02} = a_{02}$ and $B_{02} = b_{02}$ we have that the continuous piecewise quadratic Hamiltonian systems (17) depends on six parameters. This number of parameters is very big in order to study all the global

phase portraits of these systems. So in this paper we restrict our attention to the subfamily of continuous piecewise quadratic Hamiltonian systems (3) which have $b_{20} = -1$ and $B_{20} = 1$.

4. Global phase portraits of systems (3)

Since the right system of the continuous piecewise quadratic Hamiltonian systems (3) becomes the left system of systems (3) throngh the transformation

$$(x, y, t, a_{20}, a_{02}, b_{02}) \to (-x, -y, t, -A_{20}, -a_{02}, -b_{02}),$$

the right and left systems have the same topological phase portraits. So we only present the analysis of the right system of (3).

Furthermore we can assume $a_{02} \geq 0$ because the right system of Hamiltonian systems (3) is invariant under the transformation

$$(x, y, t, a_{20}, a_{02}, b_{02}) \to (x, -y, -t, -a_{20}, -a_{02}, b_{02}).$$

Thus we study these phase portraits in two different cases $a_{02} = 0$ and $a_{02} > 0$.

4.1. *The phase portraits when* $a_{02} = 0$

The continuous piecewise quadratic Hamiltonian systems (3) become

$$\begin{pmatrix} \dot{x} \\ \dot{y} \end{pmatrix} = \begin{cases} \begin{pmatrix} y + a_{20}x^2 - 2b_{02}xy \\ -x^2 - 2a_{20}xy + b_{02}y^2 \end{pmatrix}, & \text{for } x \geq 0, \\ \begin{pmatrix} y + A_{20}x^2 - 2b_{02}xy \\ x^2 - 2A_{20}xy + b_{02}y^2 \end{pmatrix}, & \text{for } x \leq 0. \end{cases} \tag{21}$$

Then we consider the infinite singular points of the right system of systems (21) using the Poincaré compactification. Since the infinite singular points at $U_1|_{v=0}$ are complicated, we first consider the origin in the local chart U_2.

In U_2 the right system of systems (21) writes

$$\dot{u} = -3b_{02}u + v + 3a_{20}u^2 + u^3, \qquad \dot{v} = -v(b_{02} - 2a_{20}u - u^2). \tag{22}$$

The origin O_1 of system (22) is a singular point, whose linear part has two eigenvalues $-b_{02}$ and $-3b_{02}$. Hence, the origin is an attracting node when $b_{02} > 0$, or a repelling node when $b_{02} < 0$, or a nilpotent singularity point when $b_{02} = 0$. Furthermore applying Theorem 3.5 of [Dumortier *et al.*, 2006] we obtain that the nilpotent point at the origin is a repelling node when $a_{20} = b_{02} = 0$, or of type E-H (i.e. the local phase portrait of this singular point is formed by one elliptic sector and one parabolic sector) when $b_{02} = 0$ and $a_{20} \neq 0$. Since the degree of systems (21) is 2, the flow in a neighborhood of the origin O_2 of V_2 has the opposite sense with respect to the flow one in U_2.

Now we consider the infinite singular points in $U_1|_{v=0}$. In the local chart U_1 the right system of systems (21) has the form

$$\dot{u} = -1 - 3a_{20}u + 3b_{02}u^2 - u^2v, \qquad \dot{v} = -v(a_{20} - 2b_{02}u + uv). \tag{23}$$

4.1.1. *Subcase* $b_{02} = 0$.

System (23) has no infinite singular points when $a_{20} = 0$, and it has one infinite singular point $(A_1, 0) = (-1/(3a_{20}), 0)$, which is an attracting node or a repelling node, when $a_{20} > 0$ or $a_{20} < 0$, respectively.

We consider the finite singular points of the right system of (21). If $a_{20} = 0$ the right system of (21) has only one finite singular point at the origin. We obtain that the phase portrait with all singular points in the right half Poincaré disc is shown in Figure 3(a).

If $a_{20} \neq 0$ the right system of (21) has two finite singular points $(0, 0)$ and $p_1 = (1/(2a_{20}^2), -1/(4a_{20}^3))$, where p_1 is a saddle. Then we obtain that the right half phase portraits with all singular points are shown in Figure 3(b) and Figure 3(c) when $a_{20} > 0$ and $a_{20} < 0$, respectively.

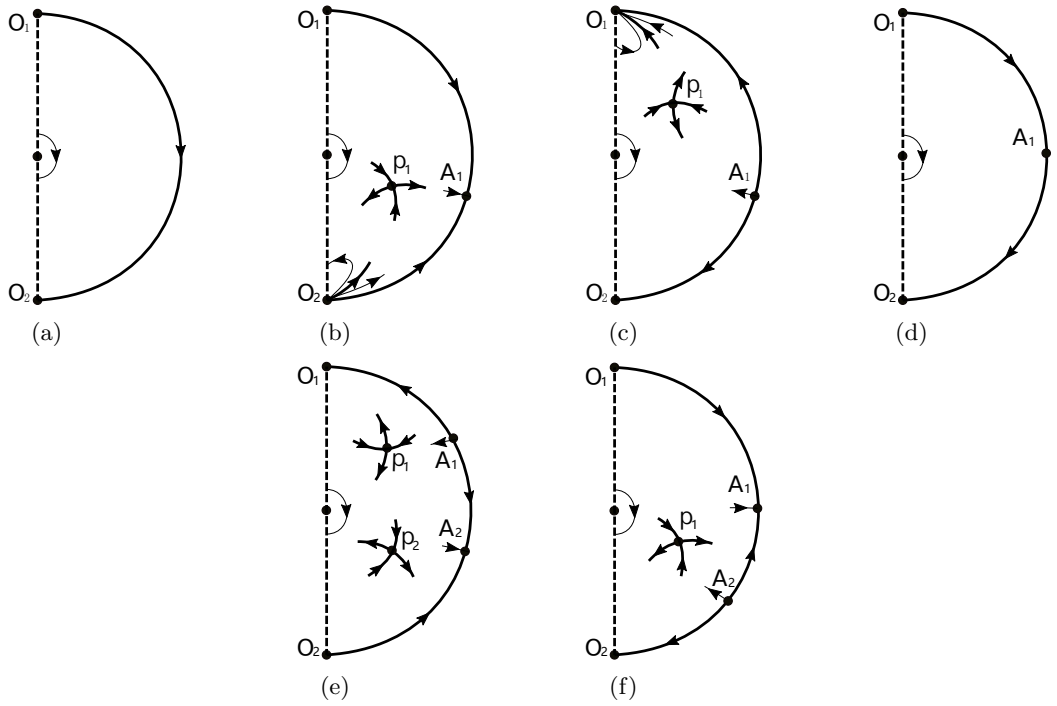

Fig. 3. The right half phase portraits with all finite and infinite singular points of systems (21).

4.1.2. *Subcase* $b_{02} \neq 0$

We separate the study of the infinite singular points at $U_1|_{v=0}$ in three cases: i) $3a_{20}^2 + 4b_{02} < 0$, ii) $3a_{20}^2 + 4b_{02} = 0$, and iii) $3a_{20}^2 + 4b_{02} > 0$.

i) If $3a_{20}^2 + 4b_{02} < 0$ system (23) has no infinite singular points.

We analyze the finite singular points of the right system of (21).

i.1) When $a_{20}^2 + b_{02} < 0$ the right system of systems (21) has only one finite singular point at origin.

i.2) When $a_{20}^2 + b_{02} = 0$ the right system of systems (21) has two possible finite singular points $(0, 0)$ and $p_1 = (-1/a_{20}^2, 1/a_{20}^3)$. Since $-1/a_{20}^2 < 0$, the singular point p_1 is a virtual singular point.

i.3) When $a_{20}^2 + b_{02} > 0$ the right system of systems (21) has three possible finite singular points $(0, 0)$, $p_1 = (x_1, y_1)$ and $p_2 = (x_2, y_2)$ where

$$x_{1,2} = \frac{1}{a_{20}^2 + 2b_{02} \pm M_1}, \qquad y_{1,2} = -\frac{a_{20}}{2a_{20}^4 + 3a_{20}^2 b_{02} \pm 2a_{20}^2 M_1 \pm 2b_{02} M_!},$$
$$M_1 = \sqrt{a_{20}^2(a_{20}^2 + b_{02})}.$$

Since $x_{1,2} < 0$ in this subcase, these two points $p_{1,2}$ are virtual singular points. In the above subcases the right half phase portrait of systems (21) is topological equivalently to the one of Figure 3(a).

ii) If $3a_{20}^2 + 4b_{02} = 0$ system (23) has one infinite singular point $(A_1, 0) = (-2/(3a_{20}), 0)$, which is of type E-H.

The right system of (21) has two singular points $(0, 0)$ and $p_1 = (-1/a_{20}^2, 2/a_{20}^3)$, but p_1 is a virtual singular point. Then we obtain that the right half phase portrait of system (21) is shown in Figure 3(d).

iii) If $3a_{20}^2 + 4b_{02} > 0$ system (23) has two infinite singular points $(A_1, 0)$ and $(A_2, 0)$, where

$$A_1 = \frac{3a_{20} + \sqrt{3(3a_{20}^2 + 4b_{02})}}{6b_{02}}, \qquad A_2 = \frac{3a_{20} - \sqrt{3(3a_{20}^2 + 4b_{02})}}{6b_{02}},$$

which are two nodes.

And the right system of systems (21) has three possible singular points $(0, 0)$, $p_1 = (x_1, y_1)$ and

$p_2 = (x_2, y_2)$. The Jacobian matrix of the right system of systems (21) at a finite singular point (x, y) is

$$\begin{pmatrix} 2(a_{20}x - b_{02}y) & 1 - 2b_{02}x \\ -2(x + a_{20}y) & -2(a_{20}x - b_{02}y) \end{pmatrix}. \tag{24}$$

Furthermore we have $a_{20}^2 + b_{02} > 0$ when $3a_{20}^2 + 4b_{02} > 0$. We claim that there are no finite singular points for the right system of systems (21) whose linear part is identically zero. Then we compute the Gröbner basis for the polynomials $\dot{x}$, $\dot{y}$, $a_{20}x - b_{02}y$ and $1 - 2b_{02}x$ is 1. We again calculate the Gröbner basis for four polynomials $\dot{x}$, $\dot{y}$, $a_{20}x - b_{02}y$ and $x + a_{20}y$, then we obtain four polynomials $(a_{20}^2 + b_{02})y$, $-y(a_{20} - b_{02}^2 y)$, $y(1 + a_{20}b_{02}y)$ and $x + a_{20}y$. From $a_{20}^2 + b_{02} > 0$ we have that the right system of systems (21) has no nilpotent singular points different from $(0, 0)$, because these four polynomials must be zero. Thus all the remaining finite singular points are hyperbolic, or semi-hyperbolic, or centers and by Theorems 2.15 and 2.19 of [Dumortier *et al.*, 2006], then the remaining finite singular points $p_{1,2}$ must be saddles or centers because this system is Hamiltonian.

By Theorem 4, on the Poincaré sphere the known singular points of the right system of (21) have total index 4. Then the sum of indices of the singular points $p_{1,2}$ must be -2. Thus $p_{1,2}$ are two saddles. Assume that $b_{02} > 0$ then we have $x_1 > 0$ and $x_2 > 0$. Furthermore we obtain the right half phase portraits of Figure 3(e). In particular, when $a_{20} = 0$ we have $x_1 = x_2 > 0$. When $-3a_{20}^2/4 < b_{02} < 0$ we have $x_1 > 0$ and $x_2 < 0$. Hence the singular point p_2 is a virtual singular point. We have the right half phase portrait of Figure 3(f).

From the above analysis we have the following result.

Proposition 1. *For the right system of systems* (21) *the following statements hold.*

(I) If either $b_{02} = 0$ *and* $a_{20} = 0$, *or* $3a_{20}^2 + 4b_{02} < 0$ *the right system of* (21) *has two infinite singular points* $O_{1,2}$, *which are a repelling node and an attracting node, respectively, and one finite singular point the* $(0, 0)$, *see Figure 3(a).*

(II) If $b_{02} = 0$ *and* $a_{20} \neq 0$ *the right system of* (21) *has three infinite singular point* $(A_1, 0) = (-1/(3a_{20}), 0)$, *which is an attracting node for* $a_{20} > 0$ *or a repelling node for* $a_{20} < 0$, *and* $O_{1,2}$, *which are of type E-H, and two finite singular points* $(0, 0)$ *and* $p_1 = (1/(2a_{20}^2), -1/(4a_{20}^3))$, *where* p_1 *is a saddle, see Figures 3(b) and 3(c).*

(III) If $b_{02} < 0$ *and* $3a_{20}^2 + 4b_{02} = 0$ *the right system of* (21) *has three infinite singular points* $(A_1, 0) = (-2/(3a_{20}), 0)$, *which is of type E-H, and* $O_{1,2}$, *which are a repelling node and an attracting node, respectively, and one finite singular point the* $(0, 0)$, *see Figure 3(d).*

(IV) If $b_{02} \neq 0$ *and* $3a_{20}^2 + 4b_{02} > 0$ *the right system of* (21) *has four infinite singular points* $(A_{1,2}, 0)$ *and* $O_{1,2}$, *which are nodes.*
(IV.1) If $b_{02} > 0$ *the right system of* (21) *has three finite singular points* $(0, 0)$, $p_1 = (x_1, y_1)$ *and* $p_2 = (x_2, y_2)$, *where* $p_{1,2}$ *are two saddles, see Figure 3(e).*
(IV.2) If $b_{02} < 0$ *the right system of* (21) *has two finite singular points* $(0, 0)$ *and* $p_1 = (x_1, y_1)$, *where* p_1 *is a saddle, see Figure 3(f).*

As in the above proposition we obtain the left half phase portrait of systems (21).

Proposition 2. *For the left system of systems* (21) *the following statements hold.*

(I) If either $b_{02} = 0$ *and* $A_{20} = 0$, *or* $3A_{20}^2 - 4b_{02} < 0$ *the left system of* (21) *has two infinite singular points* $O_{1,2}$, *which are an attracting node and a repelling node, respectively, and one finite singular point the* $(0, 0)$, *whose phase portraits are topologically equivalent to the ones of Figure 3(a).*

(II) If $b_{02} = 0$ *and* $A_{20} \neq 0$ *the left system of* (21) *has three infinite singular points* $(B_1, 0) = (1/(3A_{20}), 0)$, *which is a repelling node for* $A_{20} > 0$ *or an attracting node for* $A_{20} < 0$, *and* $O_{1,2}$, *which are of type E-H, and two finite singular points the* $(0, 0)$ *and* $p_1^* = (-1/(2A_{20}^2), -1/(4A_{20}^3))$, *where* p_1^* *is a saddle, whose phase portraits are topologically equivalent to the ones of Figures 3(b) or 3(c).*

(III) If $b_{02} > 0$ *and* $3A_{20}^2 - 4b_{02} = 0$ *the left system of* (21) *has three infinite singular points* $(B_1, 0) = (2/(3A_{20}), 0)$, *which is of type E-H, and* $O_{1,2}$, *which are an attracting node and a repelling node,*

respectively, and one finite singular point the $(0,0)$*, whose phase portraits are topologically equivalent to the ones of Figure 3(d).*

(IV) If $b_{02} \neq 0$ *and* $3A_{20}^2 - 4b_{02} > 0$ *the left system of* (21) *has four infinite singular points* $(B_{1,2}, 0)$ *and* $O_{1,2}$*, which are four nodes.*

(IV.1) If $b_{02} < 0$ *the left system of* (21) *has three finite singular points* $(0,0)$*,* $p_1^* = (x_1^*, y_1^*)$ *and* $p_2^* = (x_2^*, y_2^*)$*, where* $p_{1,2}^*$ *are two saddles, whose phase portraits are topologically equivalent to the ones of Figure 3(e).*

(IV.2) If $b_{02} > 0$ *the left system of* (21) *has two finite singular points* $(0,0)$ *and* $p_1^* = (x_1^*, y_1^*)$*, where* p_1^* *is a saddle, whose phase portraits are topologically equivalent to the ones of Figure 3(f). Here*

$$B_1 = \frac{3A_{20} + \sqrt{3(3A_{20}^2 - 4b_{02})}}{6b_{02}}, \qquad B_2 = \frac{3A_{20} - \sqrt{3(3A_{20}^2 - 4b_{02})}}{6b_{02}},$$
$$x_{1,2}^* = -\frac{1}{A_{20}^2 - 2b_{02} \pm M_2}, \qquad y_{1,2}^* = -\frac{A_{20}}{2A_{20}^4 - 3A_{20}^2 b_{02} \pm 2A_{20}^2 M_2 \mp 2b_{02} M_2},$$
$$M_2 = \sqrt{A_{20}^2(A_{20}^2 - b_{02})}.$$

Proposition 3. *The phase portraits of systems* (3) *with* $a_{02} = 0$ *are topologically equivalent to the 12 phase portraits showed in Figure 1, in Table 1 we provide the values of the parameters which realize the different phase portraits.*

Right system		Left system	Phase portraits
$b_{02} = 0$	$a_{20} = 0$	$A_{20} = 0$	1.1
		$A_{20} \neq 0$	1.2
	$a_{20} \neq 0$	$A_{20} = 0$	1.2
		$A_{20} = -a_{20}$	1.3
		$a_{20}A_{20} < 0$, $A_{20} \neq -a_{20}$	1.4
		$A_{20} = a_{20}$	1.5
		$a_{20}A_{20} > 0$, $A_{20} \neq a_{20}$	1.6
$b_{02} < 0$	$3a_{20}^2 + 4b_{02} < 0$	$A_{20} = 0$	1.3
		$A_{20} \neq 0$	1.4
	$3a_{20}^2 + 4b_{02} = 0$	$A_{20} = 0$	1.7
		$A_{20} \neq 0$	1.8
	$3a_{20}^2 + 4b_{02} > 0$	$A_{20} = 0$	1.10-1.12
		$A_{20} \neq 0$	1.9-1.11
$b_{02} > 0$	$a_{20} = 0$	$3A_{20}^2 - 4b_{02} < 0$	1.3
		$3A_{20}^2 - 4b_{02} = 0$	1.7
		$3A_{20}^2 - 4b_{02} > 0$	1.10-1.12
	$a_{20} \neq 0$	$3A_{20}^2 - 4b_{02} < 0$	1.4
		$3A_{20}^2 - 4b_{02} = 0$	1.8
		$3A_{20}^2 - 4b_{02} > 0$	1.9-1.11

Table 1. The conditions for the phase portraits of systems (3) with $a_{02} = 0$.

Proof. We just prove subcases 1.1,1.9-1.12, because the proof of the other phase portraits follow from Propositions 1 and 2.

(a) For the case $a_{20} = b_{02} = A_{20} = 0$ systems (21) have one finite singular point the $(0,0)$, which is a center, and two infinite singular points $O_{1,2}$. The infinity singular points $O_{1,2}$ in the right system of systems (21) are a repelling node and an attracting node, respectively. And these two singular points in the left system of systems (21) are an attracting node and a repelling node, respectively. Then the infinity singular points $O_{1,2}$ in systems (21) are both formed by one parabolic sector, which comes from the combination of two nodes. Hence we obtain the phase portrait 1.1 of Figure 1.

(b) For the case $b_{02} > 0$, $a_{20} \neq 0$ and $3A_{20}^2 - 4b_{02} > 0$ systems (21) have six nodes $(A_1, 0)$, $(A_2, 0)$, $(B_1, 0)$, $(B_2, 0)$, O_1 and O_2 at infinity, and four finite singular points, i.e. the center $(0,0)$, three saddles

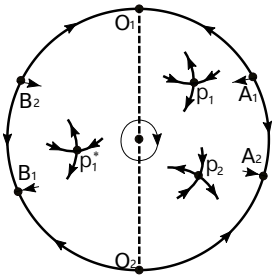

Fig. 4. The local phase portraits with all finite and infinite singular points of systems (21) with $b_{02} > 0$ and $3A_{20}^2 - 4b_{02} > 0$.

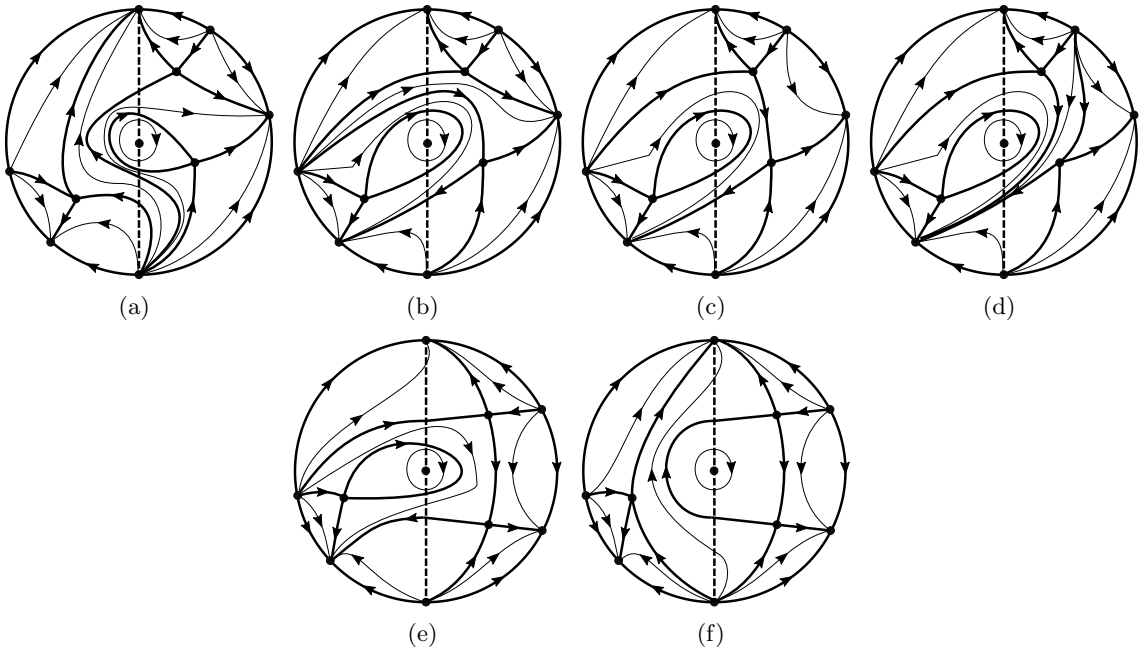

Fig. 5. The possible phase portraits of systems (21).

$p_{1,2} = (x_{1,2}, y_{1,2})$ and $p_1^* = (x_1^*, y_1^*)$, see Figure 4.

Since the finite singular points of the piecewise differential systems (21) are saddle, center or cusp there must be a saddle or a cusp in the boundary of the period annulus of center.

(b.1) We assume that p_2 is in the boundary of the period annulus of the origin, creating a center-loop. If the separatrices of p_1 connect with the infinite singular points O_1, $(A_1, 0)$, $(A_2, 0)$ and $(B_1, 0)$, respectively, then the separatrices of p_1^* must connect with the infinite singular points O_2, $(A_2, 0)$, $(B_1, 0)$ and $(B_2, 0)$, respectively. Thus we obtain the phase portrait 1.9 of Figure 1, which can be realized when $a_{20} = 1$, $b_{02} = 2$ and $A_{20} = 2$.

If the separatrices of p_1^* connect with the infinite singular points O_1, O_2, $(B_1, 0)$ and $(B_2, 0)$, respectively. Then the separatrices of p_1 connect with the infinite singular points O_1, O_2, $(A_1, 0)$ and $(A_2, 0)$, respectively. Then we have the phase portrait of Figure 5(a), which can be realized when $a_{20} = 0.1$, $b_{02} = 1$ and $A_{20} = 1.3$. Since the separatrix skeleton of this phase portrait is equivalent with the one of phase portrait 1.9 of Figure 1, by Theorem 2, they are topologically equivalent. From these two phase portraits it follows by the continuity of the phase portraits with respect to the parameters must exist one phase portrait such that one separatrix of the saddle p_1 connects with one separatrix of the saddle p_1^*, providing the phase portrait 1.10 of Figure 1.

(b.2) Similarly assume that p_1^* is in the boundary of the period annulus of the origin, creating a center-loop, then we have the phase portraits of Figures 5(b)-5(d), which are topologically equivalent to 1.9-1.10

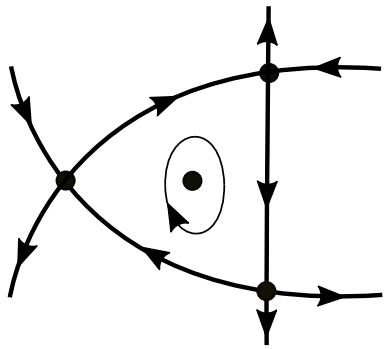

Fig. 6. A tri-heteroclinic loop.

of Figure 1, respectively. From the phase portrait 1.9 and the phase portrait of Figure 5(b), it follows by the continuity of the phase portraits with respect to the parameters that two separatrices of the saddle p_2 will connect with two separatrices of the saddle p_1^* producing a heteroclinic loop. Thus we obtain the phase portrait 1.11 of Figure 1.

(b.3) Assume that p_1 is in the boundary of the period annulus of the origin we also have the phase portraits, which are topologically equivalent to the phase portraits 1.9-1.11 of Figure 1.

(c) For the case $b_{02} > 0$, $a_{20} = 0$ and $3A_{20}^2 - 4b_{02} > 0$ systems (21) also have the above six infinite singular points $(A_{1,2}, 0)$, $(B_{1,2}, 0)$ and $O_{1,2}$, and four finite singular points $(0, 0)$, $p_{1,2}$ and p_1^*, where $p_1 = (1/(2b_{02}), 1/(2b_{02}\sqrt{b_{02}}))$, $p_2 = (1/(2b_{02}), -1/(2b_{02}\sqrt{b_{02}}))$, see Figure 4. Since $H^+(x,y)|_{p_1} = H^+(x,y)|_{p_2} = 1/(24b_{02}^3)$ we have that the saddles p_1 and p_2 are on the same energy level. If p_1^* is in the boundary of the period annulus of the origin, we have the phase portrait of Figure 5(e), which is realized when $a_{20} = 0$, $b_{02} = 1$ and $A_{20} = 2$. In this subcase the phase portrait is topologically equivalent to the phase portraits 1.10 of Figure 1.

If the saddles p_1 and p_2 are in the boundary of the period annulus of the origin, producing a heteroclinic loop, we have the phase portrait of Figure 5(f), which is realized when $a_{20} = 0$, $b_{02} = 2$ and $A_{20} = 2$. This phase portrait is topologically equivalent to 1.11 of Figure 1. From the phase portraits in Figures 5(e) and 5(f) it follows by the continuity of the phase portraits with respect to the parameters b_{02} and A_{20} that the three saddles $p_{1,2}$ and p_1^* are in the boundary of the period annulus of the origin, which produces a tri-heteroclinic loop, see Figure 6. Then we have the phase portrait 1.12 of Figure 1. ■

4.2. *The phase portraits when* $a_{02} > 0$.

We first consider the origin in the local chart U_2 of the right system of systems (3), the system becomes

$$\dot{u} = a_{02} - 3b_{02}u + v + 3a_{20}u^2 + u^3, \qquad \dot{v} = -v(b_{02} - 2a_{20}u - u^2). \tag{25}$$

The origin of system (25) is not a singular point. Note that $\dot{u}|_{v=0} = a_{02} + O(u)$ showing that the flow is increasing in the direction u.

In the local chart U_1 the right system of systems (3) has the form

$$\dot{u} = -1 - 3a_{20}u + 3b_{02}u^2 - a_{02}u^3 - u^2v, \qquad \dot{v} = -v(a_{20} - 2b_{02}u + a_{02}u^2 + uv). \tag{26}$$

Similarly we consider the following two subcases $b_{02} = 0$ and $b_{02} \neq 0$.

4.2.1. *Subcase* $b_{02} = 0$.

System (26) has at most three infinite singular points. And the Jacobian matrix of system (26) at $(u, 0)$ is given by

$$J = \begin{pmatrix} -3(a_{20} + a_{02}u^2) & -u^2 \\ 0 & -(a_{20} + a_{02}u^2) \end{pmatrix}, \tag{27}$$

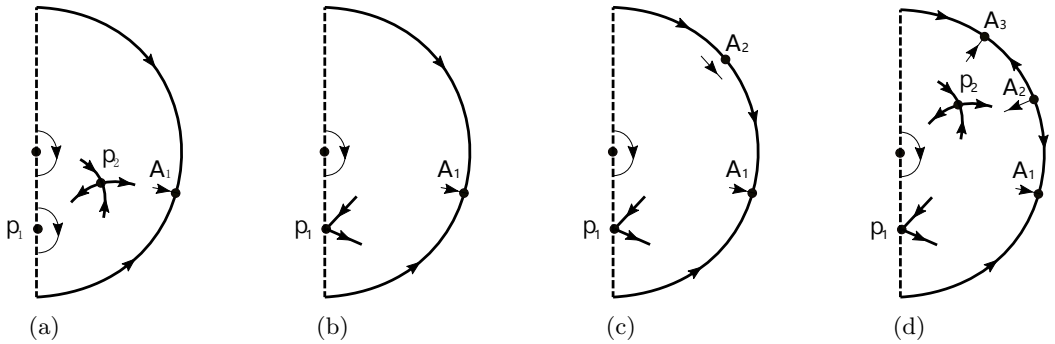

Fig. 7. The right half phase portraits with all finite and infinite singular points of systems (3) with $a_{02} > 0$ and $b_{02} = 0$.

which has a pair of eigenvalues with same sign. For analyze the infinite singular points we compute the Gröbner basis for $u'|_{v=0} = -1 - 3a_{20}u - a_{02}u^3$ and $a_{20} + a_{02}u^2$, then we obtain three polynomials

$$a_{02} + 4a_{20}^3, \qquad -2a_{20}^2 + a_{02}u, \qquad 1 + 2a_{20}u. \tag{28}$$

Hence system (26) has one nilpotent infinite singular point when $a_{02} = -4a_{20}^3$.

From $u'|_{v=0} = 0$ we obtain that if $a_{02} + 4a_{20}^3 > 0$ system (26) has one infinite singular point

$$(A_1, 0) = \left(\frac{2a_{02}a_{20} - \sqrt[3]{2(a_{02}^2 + \sqrt{a_{02}^3(a_{02} + 4a_{20}^3)})^2}}{a_{02}\sqrt[3]{4(a_{02}^2 + \sqrt{a_{02}^3(a_{02} + 4a_{20}^3)})}}, 0 \right),$$

which is an attracting node. Assume that $a_{20} > 0$ then the right system of systems (3) has three finite singular points $(0, 0)$, $p_1 = (0, -1/a_{02})$ and $p_2 = (2a_{20}/(a_{02} + 4a_{20}^3), -1/(a_{02} + 4a_{20}^3))$, where p_1 is a center and p_2 is a saddle. We have that the right half phase portrait with all singular points of systems (3) in the Poincaré disc is topologically equivalent to Figure 7(a). When $a_{20} = 0$ the singular points p_1 and p_2 collide providing a cusp. We obtain the right half phase portrait of Figure 7(b). Assuming $a_{20} < 0$ the singular point p_1 is a saddle and p_2 is a virtual singular point. This right half phase portrait is topological equivalent to phase portrait in Figure 7(b).

If $a_{02} + 4a_{20}^3 = 0$ system (26) has two infinite singular points $(A_1, 0) = (1/a_{20}, 0)$ and $(A_2, 0) = (-1/(2a_{20}), 0)$, where one is an attracting node and the other is a nilpotent point of type E-H, respectively. And the right system of systems (3) has two finite singular points $(0, 0)$ and $p_1 = (0, -1/(4a_{20}^3))$, where p_1 is a saddle. We have that the right half phase portrait of systems (3) is topologically equivalent to Figure 7(c).

If $a_{02} + 4a_{20}^3 < 0$ system (26) has three infinite singular points $(A_{1,2,3}, 0)$, which are two attracting nodes and a repelling node. The explicit expressions of $A_{2,3}$ in terms of parameter a_{20}, a_{02} and b_{02} are big and we do not provide them here. And the right system of systems (3) has three finite singular points $(0, 0)$ and $p_1 = (0, -1/a_{02})$ and $p_2 = (2a_{20}/(a_{02} + 4a_{20}^3), -1/(a_{02} + 4a_{20}^3))$, where $p_{1,2}$ are two saddles. Then we obtain right half phase portrait of Figure 7(d).

4.2.2. *Subcase* $b_{02} \neq 0$.

From $\dot{u}|_{v=0} = 1 + 3a_{20}u + 3b_{02}u^2 - a_{02}u^3 = 0$ we obtain that system (26) has one infinite singular point when either $a_{02} = a_{20}^3$ and $b_{02} = -a_{20}^2$, or $D_1 = a_{02} + 4a_{02}a_{20}^3 + 6a_{02}a_{20}b_{02} - 3a_{20}^2b_{02}^2 - 4b_{02}^3 > 0$. And system (26) has two and three infinite singular points when $D_1 = 0$ and $D_1 < 0$, respectively. The Jacobian matrix of system (26) at $(u, 0)$ is

$$J = \begin{pmatrix} -3(a_{20} - 2b_{02}u + a_{02}u^2) & -u^2 \\ 0 & -(a_{20} - 2b_{02}u + a_{02}u^2) \end{pmatrix}, \tag{29}$$

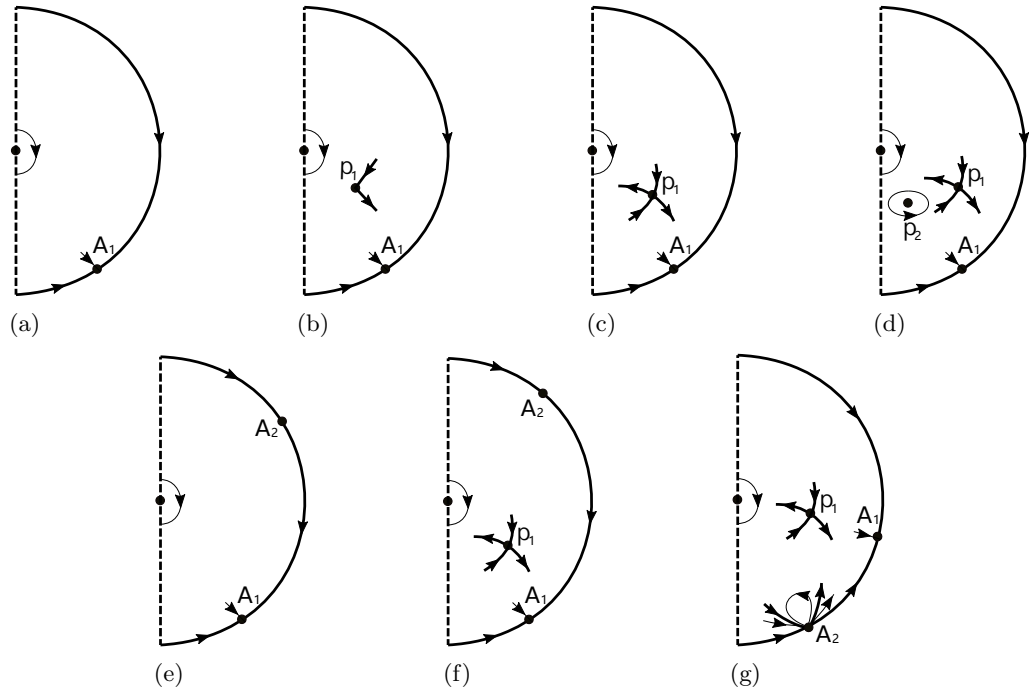

Fig. 8. The right half phase portraits with all finite and infinite singular points of systems (3) with $a_{02} > 0$ and $b_{02} \neq 0$.

which has a pair of eigenvalues with the same sign. And we compute the Gröbner basis for $\dot{u}|_{v=0}$ and $a_{20} - 2b_{02}u + a_{02}u^2$, and obtain six polynomials

$$\begin{aligned} &D_1, \qquad -4a_{02}a_{20}^2 - 5a_{02}b_{02} - a_{20}b_{02}^2 + 2(a_{02}^2 + b_{02}^3)u, \\ &a_{02} + a_{20}b_{02} + 2(a_{20}a_{02} - b_{02}^2)u, \qquad a_{20} - 2b_{02}u + a_{02}u^2, \\ &-2a_{20}^2 - 2b_{02} + (a_{02} + a_{20}b_{02})u, \qquad -1 - 2a_{20}u + b_{02}u^2. \end{aligned} \tag{30}$$

Thus one infinite singular point of system (26) is nilpotent when $D_1 = 0$.

We consider the finite singular points of the right system of systems (3). We compute the Gröbner basis for $\dot{x}$ and $\dot{y}$ with respect to x and y, and obtain nine polynomials, and the following two

$$\begin{aligned} &a_{02}x^2 + a_{20}b_{02}x^2 + b_{02}y + 2a_{20}a_{02}xy - 2b_{02}^2xy, \\ &-x^2\{b_{02} + [2a_{20}a_{02} - 2b_{02}(a_{20}^2 + 2b_{02})]x - D_1x^2\}, \end{aligned} \tag{31}$$

are enough for the analysis. Then we obtain that the right system of systems (3) has at most two finite singular points other than $(0, 0)$. The Jacobian matrix of the right system of systems (3) at a finite singular point (x, y) is

$$\begin{pmatrix} 2(a_{20}x - b_{02}y) & 1 - 2b_{02}x + 2a_{02}y \\ -2(x + a_{20}y) & -2(a_{20}x - b_{02}y) \end{pmatrix}. \tag{32}$$

We claim that there are no finite singular points for the right system of systems (3) whose linear part is identically zero. Indeed, we obtain that $a_{20}x - b_{02}y$ and $1 - 2b_{02}x + 2a_{02}y$ have no common solutions, because the Gröbner basis for the polynomials $\dot{x}$, $\dot{y}$, $a_{20}x - b_{02}y$ and $1 - 2b_{02}x + 2a_{02}y$ is 1. We again calculate the Gröbner basis for four polynomials $\dot{x}$, $\dot{y}$, $a_{20}x - b_{02}y$ and $x + a_{20}y$, then we obtain five polynomials $(a_{20}^2 + b_{02})y$, $y(a_{02} - a_{20}b_{02} + a_{02}^2y + b_{02}^3y)$, $y(a_{20} + a_{02}a_{20}y - b_{02}^2y)$, $y(1 + a_{02}y + a_{20}b_{02}y)$ and $x + a_{20}y$. It means that when $a_{20}^2 + b_{02} = 0$ it has a nilpotent singular point different from $(0, 0)$, because these five polynomials must be zero. Otherwise all the remaining finite singular points must be saddles or centers.

i) If $a_{02} = a_{20}^3$ and $b_{02} = -a_{20}^2$ the right system of systems (3) has a nilpotent infinite singular point $(A_1, 0) = (-1/a_{20}, 0)$, which is a node, and a finite singular point at the origin, whose right half phase portrait is topologically equivalent to Figure 8(a).

ii) If $D_1 > 0$ system (26) has an infinite singular point

$$(A_1, 0) = \left(\frac{1}{2a_{02}} \left[2b_{02} + \frac{2\sqrt[3]{2}(a_{02}a_{20} - b_{02}^2)}{\sqrt[3]{M_3 + \sqrt{a_{02}^2 D_1}}} - \sqrt[3]{4(M_3 + \sqrt{a_{02}^2 D_1})} \right], 0 \right),$$

where $M_3 = a_{02}^2 + 3a_{02}a_{20}b_{02} - 2b_{02}^3$, and this infinite singular point is an attracting node.

ii.1) Assume that $a_{20}^2 + b_{02} < 0$, i.e. $b_{02} < 0$ and $-\sqrt{-b_{02}} < a_{20} < \sqrt{-b_{02}}$, the right system of systems (3) has only one finite singular point the $(0, 0)$. We have that the right half phase portrait in the Poincaré disc is topologically equivalent to Figure 8(a).

ii.2) Assuming $a_{20}^2 + b_{02} = 0$ then the right system of systems (3) has two possible finite singular points $(0, 0)$ and $p_1 = (a_{20}/(a_{02} - a_{20}^3), -1/(a_{02} - a_{20}^3))$.

ii.2.1) When $a_{20}/(a_{02} - a_{20}^3) < 0$, i.e either $b_{02} < 0$, $a_{02} < \sqrt{-b_{02}^3}$ and $a_{20} = \sqrt{-b_{02}}$, or $b_{02} < 0$ and $a_{20} = -\sqrt{-b_{02}}$ the singular point p_1 is a virtual singular point. The right half phase portrait with all singular points in the Poincaré disc is topologically equivalent to Figure 8(a).

ii.2.2) When $a_{20}/(a_{02} - a_{20}^3) > 0$, i.e $b_{02} < 0$, $a_{02} > \sqrt{-b_{02}^3}$ and $a_{20} = \sqrt{-b_{02}}$ the singular point p_1 is a cusp. Hence we have the right half phase portrait of Figure 8(b).

ii.3) Assuming $a_{20}^2 + b_{02} > 0$ the right system of systems (3) has two possible singular points $p_{1,2} = (x_{1,2}, y_{1,2})$ other than $(0, 0)$, where

$$\begin{aligned} x_{1,2} &= \frac{a_{02}a_{20} - a_{20}^2 b_{02} - 2b_{02}^2 \mp (a_{02} + a_{20}b_{02})\sqrt{a_{20}^2 + b_{02}}}{D_1}, \\ y_{1,2} &= -\frac{a_{02} + 2a_{20}^3 + 3a_{20}b_{02} \pm 2(a_{20}^2 + b_{02})\sqrt{a_{20}^2 + b_{02}}}{D_1}. \end{aligned} \tag{33}$$

By Theorem 4 the sum of indices of $p_{1,2}$ must be 0, thus $p_{1,2}$ are a saddle and a center. We denote by $\mathrm{R}[f(\alpha), i]$ the i-th real root of the polynomial $f(\alpha)$ with respect to α, and these roots are ordered as follows $\mathrm{R}[f(\alpha), i] < \mathrm{R}[f(\alpha), j]$ if and only if $i < j$. Then we have the following subcases.

ii.3.1) When $x_1 < 0$ and $x_2 < 0$, i.e. either $b_{02} < 0$ and $\mathrm{R}[D_1, 1] < a_{20} < -\sqrt{-b_{02}}$, or $b_{02} < 0$, $a_{02} < \sqrt{-b_{02}^3}$ and $\sqrt{-b_{02}} < a_{20} < \mathrm{R}[D_1, 2]$, the points $p_{1,2}$ are two virtual singular points. The right half phase portrait in this subcase is topologically equivalent to the ones of Figure 8(a).

ii.3.2) When $x_1 < 0$ and $x_2 > 0$, i.e. $b_{02} > 0$ and $a_{20} > \mathrm{R}[D_1, 1]$, the point p_2 is a virtual singular point. The right half phase portrait is topological equivalent to Figure 8(c).

ii.3.3) When $x_1 > 0$ and $x_2 > 0$, i.e. either $b_{02} < 0$, $a_{02} < \sqrt{-b_{02}^3}$ and $a_{20} > \mathrm{R}[D_1, 3]$, or $b_{02} < 0$, $a_{02} \geq \sqrt{-b_{02}^3}$ and $a_{20} > \sqrt{-b_{02}}$, we have the right half phase portrait of Figure 8(d).

iii) If $D_1 = 0$ system (26) has two infinite singular points $(A_1, 0)$ and $(A_2, 0)$, which are an attracting node and a nilpotent point of type E-H. And the right system of systems (3) has one possible finite singular point

$$p_1 = \left(-\frac{b_{02}}{2a_{02}a_{20} - 2b_{02}(a_{20}^2 + 2b_{02})}, -\frac{a_{02} + a_{20}b_{02}}{4(a_{20}^2 + b_{02})(-a_{02}a_{20} + a_{20}^2 b_{02} + 2b_{02}^2)} \right)$$

other than the origin, where p_1 is a saddle.

iii.1) When $b_{02}/(a_{02}a_{20} - a_{20}^2 b_{02} - 2b_{02}^2) > 0$, i.e. either $b_{02} < 0$ and $a_{20} = \mathrm{R}[D_1, 1]$, or $b_{02} < 0$, $a_{02} < \sqrt{-b_{02}^3}$ and $a_{20} = \mathrm{R}[D_1, 2]$, the point p_1 is a virtual singular point. We obtain the right half phase portrait of Figure 8(e).

iii.2) When $b_{02}/(a_{02}a_{20} - a_{20}^2 b_{02} - 2b_{02}^2) < 0$, i.e. either $b_{02} < 0$, $a_{02} < \sqrt{-b_{02}^3}$ and $a_{20} = \mathrm{R}[D_1, 3]$, or $b_{02} > 0$ and $a_{20} = \mathrm{R}[D_1, 1]$, we have that the right half phase portrait in the Poincaré disc is topologically equivalent to Figure 8(f) or 8(g).

iv) If $D_1 < 0$ system (26) has three infinite singular points $(A_{1,2,3}, 0)$, which are two attracting nodes and one repelling node. And the right system of systems (3) has two possible singular points $p_{1,2} = (x_{1,2}, y_{1,2})$ different from the origin. By Theorem 4 on the Poincaré sphere the sum of indices of $p_{1,2}$ must be -2, thus, $p_{1,2}$ are two saddles. Then we have only the following two subcases.

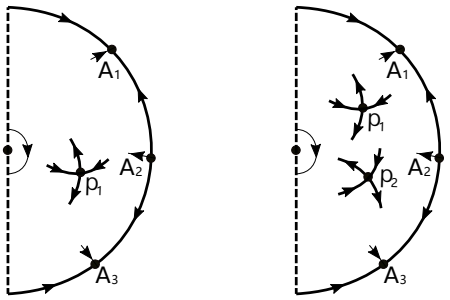

(a) (b)

Fig. 9. The right half phase portraits with all finite and infinite singular points of systems (3) with $a_{02} > 0$ and $b_{02} = 0$.

iv.1) When $x_1x_2 < 0$, i.e. either $b_{02} < 0$, $a_{02} < \sqrt{-b_{02}^3}$ and $\mathrm{R}[D_1, 2] < a_{20} < \mathrm{R}[D_1, 3]$, or $b_{02} < 0$ and $a_{20} < \mathrm{R}[D_1, 1]$, one of the points $p_{1,2}$ is virtual. Then we have that the right half phase portrait in the Poincaré disc is topologically equivalent to the ones of Figure 9(a).

iv.2) When $x_1 > 0$ and $x_2 > 0$, i.e. $b_{02} > 0$ and $a_{20} < \mathrm{R}[D_1, 1]$, we have the right half phase portrait of Figure 9(b).

Then we have the following results.

Proposition 4. *For the right system of systems* (3) *the following statements hold.*

(I) If $b_{02} = 0$ and $a_{02} + 4a_{20}^3 > 0$ the right system of systems (3) *has one infinite singular point $(A_1, 0)$, which is an attracting node.*
(I.1) If $a_{20} > 0$ the right system of systems (3) *has three finite singular points $(0, 0)$, $p_1 = (0, -1/a_{02})$ and $p_2 = (2a_{20}/(a_{02} + 4a_{20}^3), -1/(a_{02} + 4a_{20}^3))$, where p_1 is a center and p_2 is a saddle, see Figure 7(a).*
(I.2) If $a_{20} \leq 0$ the right system of systems (3) *has two finite singular points $(0, 0)$ and $p_1 = (0, -1/a_{02})$, where p_1 is a saddle, see Figure 7(b).*

(II) If $b_{02} = 0$ and $a_{02} + 4a_{20}^3 = 0$ the right system of systems (3) *has two infinite singular points $(A_1, 0) = (1/a_{20}, 0)$, $(A_2, 0) = (-1/(2a_{20}), 0)$, which are an attracting node and a point of type E-H, respectively, and two finite singular point $(0, 0)$ and $p_1 = (0, -1/a_{02})$, where p_1 is a saddle see Figure 7(c).*

(III) If $b_{02} = 0$ and $a_{02} + 4a_{20}^3 < 0$ the right system of systems (3) *has three infinite singular points $(A_{1,2,3}, 0)$, which are a repelling node and two attracting nodes, and three finite singular points $(0, 0)$ and $p_{1,2}$, where $p_{1,2}$ are two saddles, see Figure 7(d).*

(IV) If either $a_{02} = a_{20}^3$ and $b_{02} = -a_{20}^2$, or $D_1 > 0$ the right system of systems (3) *has an infinite singular point $(A_1, 0)$, which is an attracting node.*
(IV.1) If either $b_{02} < 0$ and $\mathrm{R}[D_1, 1] < a_{20} < \sqrt{-b_{02}}$, or $b_{02} < 0$, $a_{02} \leq \sqrt{-b_{02}^3}$ and $\sqrt{-b_{02}} \leq a_{20} < \mathrm{R}[D_1, 2]$, the right system of systems (3) *has one finite singular point $(0, 0)$, see Figure 8(a).*
(IV.2) If $b_{02} < 0$, $a_{02} > \sqrt{-b_{02}^3}$ and $a_{20} = \sqrt{-b_{02}}$ the right system of systems (3) *has two finite singular points $(0, 0)$ and $p_1 = (a_{20}/(a_{02} - a_{20}^3), -1/(a_{02} - a_{20}^3))$, where p_1 is a cusp, see Figure 8(b).*
(IV.3) If $b_{02} > 0$ and $a_{20} > \mathrm{R}[D_1, 1]$ the right system of systems (3) *has two finite singular points $(0, 0)$ and $p_1 = (x_1, y_1)$, where p_1 is a saddle, see Figure 8(c).*
(IV.4) If either $b_{02} < 0$, $a_{02} < \sqrt{-b_{02}^3}$ and $a_{20} > \mathrm{R}[D_1, 3]$, or $b_{02} < 0$, $a_{02} \geq \sqrt{-b_{02}^3}$ and $a_{20} > \sqrt{-b_{02}}$ the right system of systems (3) *has three finite singular points $(0, 0)$ and $p_{1,2} = (x_{1,2}, y_{1,2})$, where p_1 is a saddle and p_2 is a center, see Figure 8(d).*

(V) If $D_1 = 0$ the right system of systems (3) *has two infinite singular points $(A_{1,2}, 0)$, which are an attracting node and a point of type E-H.*
(V.1) If either $b_{02} < 0$ and $a_{20} = \mathrm{R}[D_1, 1]$, or $b_{02} < 0$, $a_{02} < \sqrt{-b_{02}^3}$ and $a_{20} = \mathrm{R}[D_1, 2]$, the right

system of systems (3) *has one finite singular point* $(0,0)$*, see Figure 8(e).*
(V.2) If either $b_{02}<0$*,* $a_{02}<\sqrt{-b_{02}^3}$ *and* $a_{20}=\mathrm{R}[D_1,3]$*, or* $b_{02}>0$ *and* $a_{20}=\mathrm{R}[D_1,1]$*, the right system of systems* (3) *has two finite singular points* $(0,0)$ *and* p_1*, where* p_1 *is a saddle, see Figures 8(f) and 8(g).*

(VI) If $D_1<0$ *the right system of systems* (3) *has three infinite nodes* $(A_{1,2,3},0)$*, which are two attracting nodes and one repelling node.*
(VI.1) If either $b_{02}<0$*,* $a_{02}<\sqrt{-b_{02}^3}$ *and* $\mathrm{R}[D_1,2]<a_{20}<\mathrm{R}[D_1,3]$*, or* $b_{02}<0$ *and* $a_{20}<\mathrm{R}[D_1,1]$*, the right system of systems* (3) *has two finite singular points* $(0,0)$ *and* $p_1=(x_1,y_1)$*, where* p_1 *is a saddle, see Figure 9(a).*
(VI.2) If $b_{02}>0$ *and* $a_{20}<\mathrm{R}[D_1,1]$ *the right system of systems* (3) *has three finite singular points* $(0,0)$ *and* $p_{1,2}=(x_{1,2},y_{1,2})$*, where* $p_{1,2}$ *are two saddles, see Figure 9(b).*

Proposition 5. *For the left system of systems* (3) *the following statements hold.*

(I) If $b_{02}=0$ *and* $a_{02}+4A_{20}^3>0$ *the left system of systems* (3) *has one infinite singular point* $(B_1,0)$*, which is a repelling node.*
(I.1) If $A_{20}>0$ *the left system of systems* (3) *has three finite singular points* $(0,0)$*,* $p_1^*=(0,-1/a_{02})$ *and* $p_2^*=-(2A_{20}/(a_{02}+4A_{20}^3),-1/(a_{02}+4A_{20}^3))$*, where* p_1^* *is a center and* p_2^* *is a saddle, whose phase portraits are topologically equivalent to the ones of Figure 7(a).*
(I.2) If $A_{20}\le 0$ *the left system of system* (3) *has two finite singular points* $(0,0)$ *and* p_1^**, where* p_1^* *is a saddle, whose phase portraits are topologically equivalent to the ones of Figure 7(b).*

(II) If $b_{02}=0$ *and* $a_{02}+4A_{20}^3=0$ *the left system of systems* (3) *has two infinite singular points* $(B_1,0)=(-1/A_{20},0)$*,* $(B_2,0)=(1/(2A_{20}),0)$*, which are a repelling node and a point type of E-H, respectively, and two finite singular points* $(0,0)$ *and* $p_1^*=(0,-1/a_{02})$*, where* p_1^* *is a saddle, whose phase portraits are topologically equivalent to the ones of Figure 7(c).*

(III) If $b_{02}=0$ *and* $a_{02}+4A_{20}^3<0$ *the left system of systems* (3) *has three infinite singular points* $(B_{1,2,3},0)$*, which are two repelling nodes and an attracting node, and three finite singular points* $(0,0)$ *and* $p_{1,2}^*$*, where* $p_{1,2}^*$ *are two saddles, whose phase portraits are topologically equivalent to the ones of Figure 7(d).*

(IV) If either $a_{02}=A_{20}^3$ *and* $b_{02}=A_{20}^2$*, or* $D_2>0$ *the left system of systems* (3) *has an infinite singular point* $(B_1,0)$*, which is a repelling node.*
(IV.1) If either $b_{02}>0$ *and* $\mathrm{R}[D_2,1]<A_{20}<\sqrt{b_{02}}$*, or* $b_{02}>0$ *and* $\sqrt{b_{02}}\le A_{20}<\mathrm{R}[D_2,2]$*, the left system of systems* (3) *has one finite singular point* $(0,0)$*, whose phase portraits are topologically equivalent to the ones of Figure 8(a).*
(IV.2) If either $b_{02}>0$*,* $a_{02}<-\sqrt{b_{02}^3}$ *and* $A_{20}=-\sqrt{b_{02}}$*, or* $b_{02}>0$*,* $a_{02}>\sqrt{b_{02}^3}$ *and* $A_{20}=\sqrt{b_{02}}$*, the left system of systems* (3) *has two finite singular points* $(0,0)$ *and* $p_1^*=(A_{20}/(A_{20}^3-a_{02}),1/(A_{20}^3-a_{02}))$*, where* p_1^* *is a cusp, whose phase portraits are topologically equivalent to the ones of Figure 8(b).*
(IV.3) If $b_{02}<0$ *and* $A_{20}>\mathrm{R}[D_2,1]$ *the left system of systems* (3) *has two finite singular points* $(0,0)$ *and* $p_1^*=(x_1^*,y_1^*)$*, where* p_1^* *is a saddle, whose phase portraits are topologically equivalent to the ones of Figure 8(c).*
(IV.4) If either $b_{02}>0$*,* $a_{02}\ge\sqrt{b_{02}^3}$ *and* $A_{20}>\sqrt{b_{02}}$*, or* $b_{02}>0$*,* $a_{02}<\sqrt{b_{02}^3}$ *and* $A_{20}>\mathrm{R}[D_2,3]$*, the left system of systems* (3) *has three finite singular points* $(0,0)$ *and* $p_{1,2}^*=(x_{1,2}^*,y_{1,2}^*)$*, where* p_1^* *is a saddle and* p_2^* *is a center, whose phase portraits are topologically equivalent to the ones of Figure 8(d).*

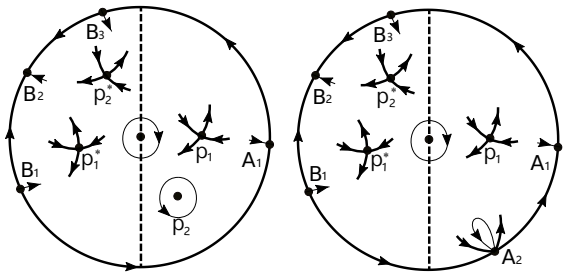

(a) (b)

Fig. 10. The local phase portraits with all finite and infinite singular points of systems (3) with (a) either $b_{02} < 0$, $a_{02} < \sqrt{-b_{02}^3}$, $a_{20} > \mathrm{R}[D_1, 3]$ and $A_{20} < \mathrm{R}[D_2, 1]$, or $b_{02} < 0$, $a_{02} > \sqrt{-b_{02}^3}$, $a_{20} > \sqrt{-b_{02}}$ and $A_{20} < \mathrm{R}[D_2, 1]$, (b) $b_{02} < 0$, $a_{02} < \sqrt{-b_{02}^3}$, $a_{20} = \mathrm{R}[D_1, 3]$ and $A_{20} < \mathrm{R}[D_2, 1]$.

Here

$$D_2 = a_{02}^2 + 4a_{02}A_{20}^3 - 6a_{02}A_{20}b_{02} - 3A_{20}^2b_{02}^2 + 4b_{02}^3,$$
$$x_{1,2}^* = -\frac{a_{02}A_{20} + A_{20}^2b_{02} - 2b_{02}^2 \pm (A_{20}b_{02} - a_{02})\sqrt{A_{20}^2 - b_{02}}}{D_2},$$
$$y_{1,2}^* = -\frac{a_{02} + 2A_{20}^3 - 3A_{20}b_{02} \pm 2\sqrt{A_{20}^2 - b_{02}}}{D_2}.$$

(V) If $D_2 = 0$ the left system of systems (3) *has two infinite singular points $(B_{1,2}, 0)$, which are a repelling node and a point of type E-H point.*
(V.1) If either $b_{02} > 0$ and $A_{20} = \mathrm{R}[D_2, 1]$, or $b_{02} > 0$, $a_{02} < \sqrt{b_{02}^3}$ and $A_{20} = \mathrm{R}[D_2, 2]$, the left system of systems (3) *has one finite singular point $(0, 0)$, whose phase portraits are topologically equivalent to the ones of Figure 8(e).*
(V.2) If either $b_{02} < 0$ and $A_{20} = \mathrm{R}[D_2, 1]$, or $b_{02} > 0$, $a_{02} < \sqrt{b_{02}^3}$ and $A_{20} = \mathrm{R}[D_2, 3]$, the left system of systems (3) *has two finite singular points $(0, 0)$ and $p_1^* = (-b_{02}/2(a_{02}A_{20} + A_{20}^2b_{02} - 2b_{02}^2), (a_{02} - A_{20}b_{02})/4(A_{20}^2 - b_{02})(a_{02}A_{20} + A_{20}^2b_{02} + 2b_{02}^2))$, where p_1^* is a saddle, whose phase portraits are topologically equivalent to the ones of Figures 8(f) or 8(g).*

(VI) If $D_1 < 0$ the left system of systems (3) *has three infinite singular points $(B_{1,2,3}, 0)$, which are two repelling nodes and an attracting node.*
(VI.1) If either $b_{02} > 0$, $a_{02} < \sqrt{b_{02}^3}$ and $\mathrm{R}[D_2, 2] < A_{20} < \mathrm{R}[D_2, 3]$, or $b_{02} > 0$ and $A_{20} < \mathrm{R}[D_2, 1]$, the left system of systems (3) *has two finite singular points $(0, 0)$ and $p_1^* = (x_1^*, y_1^*)$, where p_1^* is a saddle, whose phase portraits are topologically equivalent to the ones of Figure 9(a).*
(VI.2) If $b_{02} < 0$ and $A_{20} < \mathrm{R}[D_2, 1]$ the left system of systems (3) *has three finite singular points $(0, 0)$ and $p_{1,2}^* = (x_{1,2}^*, y_{1,2}^*)$, where $p_{1,2}^*$ are two saddles, whose phase portraits are topologically equivalent to the ones of Figure 9(b).*

Proposition 6. *The phase portraits of systems* (3) *with $a_{02} > 0$ are topologically equivalent to 37 phase portraits of Figures 1 and 2, the corresponding conditions realizing these phase portraits are given in Tables 2 and 3.*

Proof. We just prove subcases 1.25-1.29 and 1.32-1.38, because the proof of the other cases follows from Propositions 4 and 5.

(a) For the subcases either $b_{02} < 0$, $a_{02} < \sqrt{-b_{02}^3}$, $a_{20} > \mathrm{R}[D_1, 3]$ and $A_{20} < \mathrm{R}[D_2, 1]$, or $b_{02} < 0$, $a_{02} > \sqrt{-b_{02}^3}$, $a_{20} > \sqrt{-b_{02}}$ and $A_{20} < \mathrm{R}[D_2, 1]$, systems (3) has four nodes $(A_1, 0)$, $(B_1, 0)$, $(B_2, 0)$ and $(B_3, 0)$ in infinity, and five finite singular points, i.e. two centers $(0, 0)$ and p_2, three saddles p_1 and $p_{1,2}^*$, see Figure 10(a).

Right system		Left system	Phase portraits
$b_{02}=0$	$a_{20}>0$	$A_{20}>0$, $A_{20}\neq a_{20}$	1.13
		$A_{20}=a_{20}$	1.14
		$a_{02}+4A_{20}^3>0$, $A_{20}\leq 0$	1.15
		$a_{02}+4A_{20}^3=0$	1.16
		$a_{02}+4A_{20}^3<0$	1.17-1.20
	$a_{20}\leq 0$, $a_{02}+4a_{20}^3>0$	$A_{20}>0$	1.15
		$a_{02}+4A_{20}^3>0$, $A_{20}\leq 0$	1.21
		$a_{02}+4A_{20}^3=0$	1.2
		$a_{02}+4A_{20}^3<0$	1.3,1.4
	$a_{02}+4a_{20}^3=0$	$A_{20}>0$	1.16
		$a_{02}+4A_{20}^3>0$, $A_{20}\leq 0$	1.2
		$a_{02}+4A_{20}^3=0$	1.22
		$a_{02}+4A_{20}^3<0$	1.7,1.8
	$a_{02}+4a_{20}^3<0$	$A_{20}>0$	1.17-1.20
		$a_{02}+4A_{20}^3>0$, $A_{20}\leq 0$	1.4
		$a_{02}+4A_{20}^3=0$	1.7,1.8
		$a_{02}+4A_{20}^3<0$	1.9-1.12
$b_{02}<0$	$\mathrm{R}[D_1,1]<a_{20}<\sqrt{-b_{02}}$ or $a_{02}\leq\sqrt{-b_{02}^3}$, $\sqrt{-b_{02}}\leq a_{20}<\mathrm{R}[D_1,2]$	$A_{20}>\mathrm{R}[D_2,1]$	1.21
		$A_{20}=\mathrm{R}[D_2,1]$	1.2
		$A_{20}<\mathrm{R}[D_2,1]$	1.3,1.4
	$a_{02}>\sqrt{-b_{02}^3}$, $a_{20}=\sqrt{-b_{02}}$	$A_{20}>\mathrm{R}[D_2,1]$	1.15
		$A_{20}=\mathrm{R}[D_2,1]$	1.16
		$A_{20}<\mathrm{R}[D_2,1]$	1.17-1.20
	$a_{02}<\sqrt{-b_{02}^3}$, $a_{20}>\mathrm{R}[D_1,3]$ or $a_{02}\geq\sqrt{-b_{02}^3}$, $a_{20}>\sqrt{-b_{02}}$	$A_{20}>\mathrm{R}[D_2,1]$	1.13,1.14
		$A_{20}=\mathrm{R}[D_2,1]$	1.23,1.24
		$A_{20}<\mathrm{R}[D_2,1]$	1.25-1.29
	$a_{20}=\mathrm{R}[D_1,1]$ or $a_{02}<\sqrt{-b_{02}^3}$, $a_{20}=\mathrm{R}[D_1,2]$	$A_{20}>\mathrm{R}[D_2,1]$	1.2
		$A_{20}=\mathrm{R}[D_2,1]$	1.22
		$A_{20}<\mathrm{R}[D_2,1]$	1.7,1.8
	$a_{02}<\sqrt{-b_{02}^3}$, $a_{20}=\mathrm{R}[D_1,3]$	$A_{20}>\mathrm{R}[D_2,1]$	1.30,1.31
		$A_{20}=\mathrm{R}[D_2,1]$	1.5,1.6
		$A_{20}<\mathrm{R}[D_2,1]$	1.32-1.38
	$a_{02}<\sqrt{-b_{02}^3}$, $\mathrm{R}[D_1,2]<a_{20}<\mathrm{R}[D_1,3]$	$A_{20}>\mathrm{R}[D_2,1]$	1.4
		$A_{20}=\mathrm{R}[D_2,1]$	1.8
		$A_{20}<\mathrm{R}[D_2,1]$	1.9-1.11

Table 2. The conditions for the phase portraits of systems (3) with $a_{02}>0$.

(a.1) We assume that the saddle p_1^* is in the boundary of the period annulus of center p_2, creating a center-loop.

(a.1.1) If the saddle p_1 is in the boundary of the period annulus of the origin, creating the second center-loop, then the separatrices of p_2^* connect with the infinite singular points $(A_1,0)$, $(B_1,0)$, $(B_2,0)$ and $(B_3,0)$, respectively. Thus we obtain the phase portraits 1.25 and 1.26 of Figure 1, which can be realized by $a_{20}=2$, $a_{02}=1$, $b_{02}=-1.5$, $A_{20}=0.5$, and $a_{20}=2$, $a_{02}=1$, $b_{02}=-1.5$, $A_{20}=-0.5$, respectively. From the phase portrait 1.25 and 1.26, it follows by the continuity of the phase portraits with respect to the parameters that there must exist one phase portrait that one separatrix of saddle p_1^* connects with one separatrix of saddle p_2^* providing the phase portrait 1.27 of Figure 1.

(a.1.2) Similarly, if the saddle p_2^* is in the boundary of the period annulus of the origin, then we have the phase portrait of Figure 12(a), which is realized when $a_{20}=1$, $a_{02}=1$, $b_{02}=-0.5$, $A_{20}=-1.5$. This phase portrait is topological equivalent to the phase portrait 1.26 of Figure 1. From the phase portrait of Figure 12(a) and the phase portrait 1.26, by the continuity of the phase portraits with respect to the parameters that there must exist one phase portrait that p_1 and p_2^* are in the boundary of the period annulus of the origin producing a heteroclinic loop, which corresponding to the phase portrait 1.28 of Figure 1.

Right system		Left system	Phase portraits
$b_{02}>0$	$a_{20}>\mathrm{R}[D_1,1]$	$\mathrm{R}[D_2,1]<A_{20}<\sqrt{b_{02}}$, or $\sqrt{b_{02}}\le A_{20}<\mathrm{R}[D_2,2]$	1.21
		$a_{02}>\sqrt{b_{02}^3}$, $A_{20}=\sqrt{b_{02}}$	1.15
		$a_{02}\ge\sqrt{b_{02}^3}$, $A_{20}>\sqrt{b_{02}}$ or $a_{02}<\sqrt{b_{02}^3}$, $A_{20}>\mathrm{R}[D_2,3]$	1.13,1.14
		$A_{20}=\mathrm{R}[D_2,1]$ or $a_{02}<\sqrt{b_{02}^3}$, $A_{20}=\mathrm{R}[D_2,2]$	1.2
		$a_{02}<\sqrt{b_{02}^3}$, $A_{20}=\mathrm{R}[D_2,3]$	1.5,1.6
		$\mathrm{R}[D_2,2]<A_{20}<\mathrm{R}[D_2,3]$ $a_{02}<\sqrt{b_{02}^3}$, or $A_{20}<\mathrm{R}[D_2,1]$	1.3,1.4
	$a_{20}=\mathrm{R}[D_1,1]$	$\mathrm{R}[D_2,1]<A_{20}<\sqrt{b_{02}}$, or $\sqrt{b_{02}}\le A_{20}<\mathrm{R}[D_2,2]$	1.2
		$a_{02}>\sqrt{b_{02}^3}$, $A_{20}=\sqrt{b_{02}}$	1.16
		$a_{02}\ge\sqrt{b_{02}^3}$, $A_{20}>\sqrt{b_{02}}$ or $a_{02}<\sqrt{b_{02}^3}$, $A_{20}>\mathrm{R}[D_2,3]$	1.23,1.24
		$A_{20}=\mathrm{R}[D_2,1]$ or $a_{02}<\sqrt{b_{02}^3}$, $A_{20}=\mathrm{R}[D_2,2]$	1.22
		$a_{02}<\sqrt{b_{02}^3}$, $A_{20}=\mathrm{R}[D_2,3]$	1.6
		$a_{02}<\sqrt{b_{02}^3}$, $\mathrm{R}[D_2,2]<A_{20}<\mathrm{R}[D_2,3]$ or $A_{20}<\mathrm{R}[D_2,1]$	1.7,1.8
	$a_{20}<\mathrm{R}[D_1,1]$	$\mathrm{R}[D_2,1]<A_{20}<\sqrt{b_{02}}$, or $\sqrt{b_{02}}\le A_{20}<\mathrm{R}[D_2,2]$	1.7,1.8
		$a_{02}>\sqrt{b_{02}^3}$, $A_{20}=\sqrt{b_{02}}$	1.17-1.20
		$a_{02}\ge\sqrt{b_{02}^3}$, $A_{20}>\sqrt{b_{02}}$ or $a_{02}<\sqrt{b_{02}^3}$, $A_{20}>\mathrm{R}[D_2,3]$	1.25-1.29
		$A_{20}=\mathrm{R}[D_2,1]$ or $a_{02}<\sqrt{b_{02}^3}$, $A_{20}=\mathrm{R}[D_2,2]$	1.7,1.8
		$a_{02}<\sqrt{b_{02}^3}$, $A_{20}=\mathrm{R}[D_2,3]$	1.32-1.38
		$a_{02}<\sqrt{b_{02}^3}$, $\mathrm{R}[D_2,2]<A_{20}<\mathrm{R}[D_2,3]$ or $A_{20}<\mathrm{R}[D_2,1]$	1.9-1.11

Table 3. The conditions for the phase portraits of systems (3) with $a_{02}>0$.

(a.2) Assume that the saddle p_1^* is in the boundary of the period annulus of the origin. Then the saddle p_1 is in the boundary of the period annulus of center p_2. Thus we have the phase portraits Figure of 12(b) and 12(c), which are realized when $a_{20}=1.3$, $a_{02}=1$, $b_{02}=-1.2$, $A_{20}=-0.1$ and $a_{20}=1.3$, $a_{02}=1$, $b_{02}=-1.2$, $A_{20}=0.1$, respectively. These two phase portraits are topological equivalent to the phase portraits 1.26 and 1.25 of Figure 1, respectively. From the phase portrait 1.25 to the phase portrait in Figure 12(c), it follows by the continuity of the phase portraits with respect to the parameters that there must exist one phase portrait that the saddles p_1 and p_1^* are in the boundary of the period annulus of the origin and the center p_2 producing a twin-heteroclinic loop, see Figure 11. Then we obtain the phase portrait 1.29 of Figure 1.

(b) For the subcases $b_{02}<0$, $a_{02}<\sqrt{-b_{02}^3}$, $a_{20}=\mathrm{R}[D_1,3]$ and $A_{20}<\mathrm{R}[D_2,1]$ systems (3) has four nodes $(A_1,0)$, $(B_1,0)$, $(B_2,0)$ and $(B_3,0)$, and a point of type E-H $(A_2,0)$ in infinity, and four finite singular points, i.e. the center $(0,0)$, three saddles p_1 and $p_{1,2}^*$, see Figure 10(b).

(b.1) Assuming that the saddle p_1^* is in the boundary of the period annulus of the origin, which can create a center-loop.

(b.1.1) If the separatrices of p_2^* connect with the infinite singular points $(A_1,0)$, $(B_1,0)$, $(B_2,0)$ and

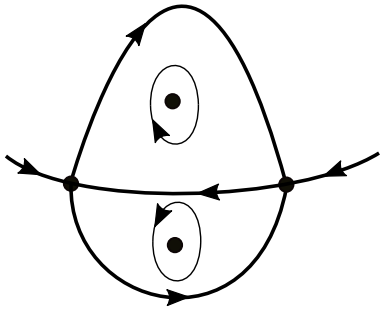

Fig. 11. A twin-heteroclinic loop.

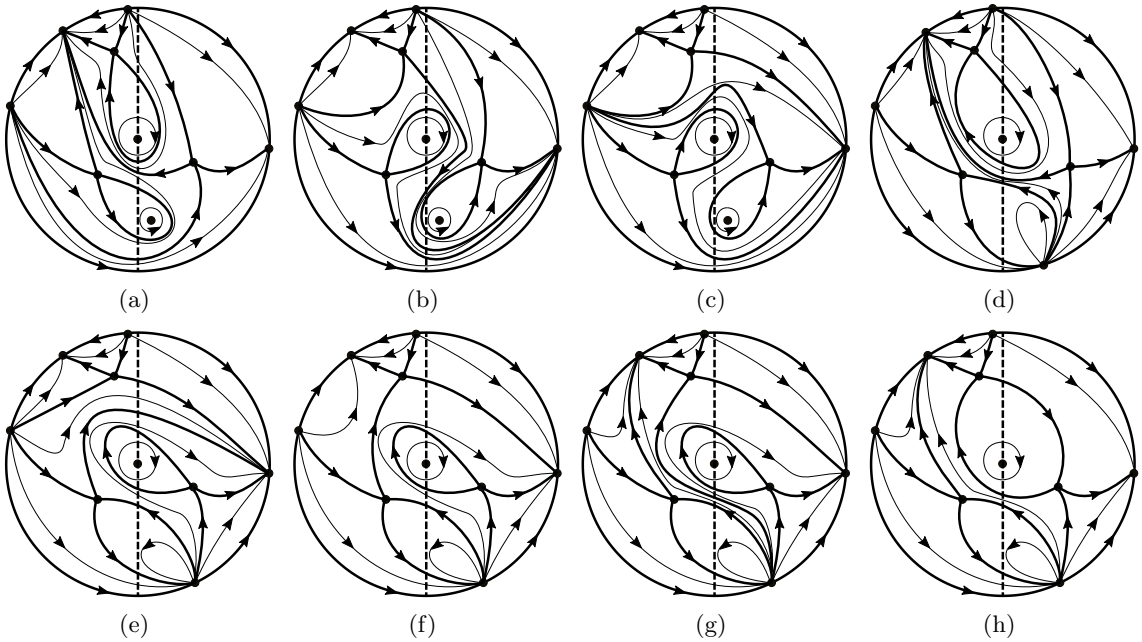

Fig. 12. The possible phase portraits of systems (3) with $a_{02} > 0$ and $b_{02} \neq 0$.

$(B_3, 0)$, respectively, then we have the phase portrait 1.32 of Figure 1. This phase portrait can be realized when $a_{20} \approx 1.27501$, $a_{02} = 1$, $b_{02} = -1.2$, $A_{20} = 0.3$.

(b.1.2) If the separatrices of p_2^* connect with the infinite singular points $(A_2, 0)$, $(B_1, 0)$, $(B_2, 0)$ and $(B_3, 0)$, respectively, the global phase portrait is topological equivalent to the phase portrait 1.34 of Figure 1. This phase portrait can be realized by taking $a_{20} \approx 1.27501$, $a_{02} = 1$, $b_{02} = -1.2$, $A_{20} = 0.1$. From the phase portrait 1.32 to 1.34, it follows by the continuity of the phase portraits that there must exist one phase portrait such that one separatrix of the saddle p_2^* connects with one separatrix of the saddle p_1, which corresponding to the ones of phase portrait 1.33 of Figure 1.

(b.2) Similarly assume that saddle p_2^* is in the boundary of the period annulus of the origin.

(b.2.1) If the separatrices of p_1^* connect with the infinite singular points $(A_2, 0)$, $(B_1, 0)$, $(B_2, 0)$ and $(B_3, 0)$, respectively, then we have the phase portrait 1.35 of Figure 1. This phase portrait can be realized when $a_{20} \approx 1.27501$, $a_{02} = 1$, $b_{02} = -1.2$, $A_{20} = -0.4$. From the phase portraits 1.34 and 1.35, by the continuity of the phase portraits with respect to the parameters, there must exist one phase portrait such that p_1^* and p_2^* are in the boundary of the period annulus of the origin producing a heteroclinic loop. Then the phase portrait is topologically equivalent to 1.36 of Figure 1.

(b.2.2) If the separatrices of p_1 connect with the infinite singular points $(A_1, 0)$, $(A_2, 0)$, $(B_2, 0)$ and $(B_3, 0)$, respectively, then we obtain the phase portrait of Figure 12(d), which is realized by taking $a_{20} \approx 1.44519$, $a_{02} = 1$, $b_{02} = -1.3$, $A_{20} = -0.5$. From the phase portrait 1.35 to the phase portrait of Figure 12(d) there must exist one phase portrait such that one separatrix of the saddle p_1 connects with one

separatrix of the saddle p_1^*, whose the phase portrait is topologically equivalent to 1.37 of Figure 1.

(b.3) Further, we assume that the saddle p_1 is in the boundary of the period annulus of the origin. Similar to the above subcases we can obtain the phase portraits of Figures 12(e)-12(h), which are topological equivalent to the phase portraits 1.32-1.34 and 1.36 of Figure 1, respectively. From the phase portrait 1.32 to the phase portrait of Figure 12(e), there must exist one phase portrait such that p_1^* and p_1 are in the boundary of the period annulus of the origin producing a heteroclinic loop, which corresponding to the phase portrait 1.38 of Figure 1. ■

Acknowledgments

The first author is partially supported by National Natural Science Foundation of China (Nos. 12001112 and 12071091), Young Innovative Talents Program in Colleges and universities of Guangdong Province (No. 2019KQNCX211) and Science and Technology Program of Guangzhou (No. 202102020443).

The second author is partially by the Agencia Estatal de Investigación grant PID2019-104658GB-I00, and the H2020 European Research Council grant MSCA-RISE-2017-777911.

References

Andronov, A., Vitt, A. & Khaikin, S. [1966] *Theory of Oscillations*, Pergamon Press, Oxford.

Artés, J. & Llibre, J. [1994] "Quadratic Hamiltonian vector fields," *J. Differential Equations* **107**, 80–95.

Aziz, W., Llibre J. & Pantazi, C. [2014] "Centers of quasi-homogeneous polynomial differential equations of degree three," *Adv. Math.* **254**, 233–250.

Banerjee, S., & Verghese, G. [2001] *Nonlinear Phenomena in Power Electronics: Attractors, Bifurcations, Chaos, and Nonlinear Control*, Wiley-IEEE Press, New York.

Bautin, N.N. [1952] "On the number of limit cycles which appear with the variation of coefficients from an equilibrium position of focus or center type," *Mat. Sb.* **30**, 181–196; *Amer. Math. Soc. Transl.* **100**, 1–19.

Chen, T., Huang, L. & Yu, P. [2021] "Center condition and bifurcation of limit cycles for quadratic switching systems with a nilpotent equilibrium point," *J. Differential Equations* **303**, 326–368.

Chen, T., Huang, L., Yu, P. & Huang, W. [2018] "Bifurcation of limit cycles at infinity in piecewise polynomial systems," *Nonlinear Anal.: Real World Appl.* **41**, 82–106.

Chen, T., Li, S. & Llibre, J. [2020] "$\mathbb{Z}_2$-equivariant linear type bi-center cubic polynomial Hamiltonian vector fields cubic system," *J. Differential Equations* **269**, 832-861.

Chen, X. & Zhang, W. [2012] "Isochronicity of centers in switching Bautin system," *J. Differential Equations* **252**, 2877–2899.

Cima, A. & Llibre, J. [1990] "Algebraic and topological classification of the homogeneous cubic vector fields in the plane," *J. Math. Anal. Appl.* **47**, 420–448.

Colak, I., Llibre, J. & Valls, C. [2014] "Hamiltonian linear type centers of linear plus cubic homogeneous polynomial vector fields," *J. Differential Equations* **257**, 1623–1661.

Colak, I., Llibre, J. & Valls, C. [2014] "Hamiltonian nilpotent centers of linear plus cubic homogeneous polynomial vector fields," *Adv. Math.* **259** (2014), 655–687.

Coll, B., Prohens, R. & Gasull, A. [1999] "The center problem for discontinuous Liénard differential equation," *Int. J. Bifurcation and Chaos* **9**, 1751–1761.

Dulac, H. [1908] "Détermination et integration d'une certaine classe d'équations différentielle ayant par point singulier un centre," *Bull. Sci. Math.* **32**, 230–252.

Dumortier, F., Llibre, J. & Artés, J. [2006] *Qualitative Theory of Planar Differential Systems* Universitext, Springer-Verlag, New York.

Filippov, A.F. [1988] *Differential Equation with Discontinuous Right-Hand Sides*, Kluwer Academic, Netherlands.

Garcia, I., Giacomini, H., Giné, J. & Llibre, J. [2016] "Analytic nilpotent centers as limits of nondegenerate centers revisited," *J. Math. Anal. Appl.* **441**, 893–899,

Gasull, A. & Torregrosa, J. [2003] "Center-focus problem for discontinuous planar differential equations," *Int. J. Bifurcation and Chaos* **13**, 1755–1765.

Guo, L., Yu, P. & Chen, Y. [2019] "Bifurcation analysis on a class of $\mathbb{Z}_2$-equivariant cubic switching systems showing eighteen limit cycles," *J. Differential Equations* **266**, 1221–1244.

Kapteyn, W. [1911] "On the midpoints of integral curves of differential equations of the first degree," *Nederl. Akad. Wetensch. Verslag. Afd. Natuurk. Konikl. Nederland* 1446–1457 (Dutch).

Kapteyn, W. [1912] "New investigations on the midpoints of integrals of differential equations of the first degree," *Nederl. Akad. Wetensch. Verslag Afd. Natuurk.* **20**, 1354–1365; **21**, 27–33 (Dutch).

Li, F., Liu, Y., Liu, Y. & Yu, P. [2018] "Bi-center problem and bifurcation of limit cycles from nilpotent singular points in Z_2-equivariant cubic vector fields," *J. Differential Equations* **265**, 4965–4992.

Liu, Y. & Li, F. [2015] "Double bifurcation of nilpotent focus," *Internat. J. Bifur. Chaos* **25**, 1550036 (10 pages).

Liu, Y. & Li, J. [2011] "Bifurcations of limit cycles created by a multiple nilpotent critical point of planar dynamical systems," *Internat. J. Bifur. Chaos* **21**, 497–504.

Lv, Y., Yuan, R. & Yu, P. [2019] "Dynamics in two nonsmooth predator-prey models with threshold harvesting," *Nonlinear Dyn.* **74**, 107–132.

Malkin, K.E. [1964] "Criteria for the center for a certain differential equation," *Volz. Mat. Sb. Vyp.* **2**, 87–91 (in Russian).

Markus, L. [1954] "Global structure of ordinary differential equations in the plane," *Trans. Amer. Math. Soc.* **76**, 127–148.

Neumann, D.A. [1975] "Classification of continuous flows on 2–manifolds," *Proc. Amer. Math. Soc.* **48**, 73–81.

Nusse,H.E. & Yorke, J.A. [1995] "Border-collision bifurcations for piecewise smooth one-dimensional maps," *Int. J. Bifurcation and Chaos* **5**, 189–207.

Peixoto, M. [1973] *Dynamical Systems, Proceedingsof a Symposium held at the University of Bahia,* Acad. Press, New York, pp.389–420.

Poincaré, H. [1881] "Mémoire sur les courbes définies par les équations différentielles, " *J. Math.* **37**, 375–422.

Schlomiuk, D. [1993] "Algebraic particular integrals, integrability and the problem of the center," *Trans. Amer. Math. Soc.* **338**, 799–841.

Stróżzyna, E. & Żołądek, H. [2012] "The analytic normal for the nilpotent singularity," *J. Differential Equations* **179**, 479–537.

Tian, Y. & Yu, P. [2015] "Center conditions in a switching Bautin system," *J. Differential Equations* **259**, 1203–1226.

Vulpe, N.I. & Sibirskii, K. S. [1988] "Centro-affine invariant conditions for the existence of a center of a differential system with cubic nonlinearities," *Dokl. Akad. Nauk. SSSR* **301**, 1297–1301 (in Russian); translation in: Soviet Math. Dokl. **38** (1989), 198–201.

Żołądek, H. [1994] "Quadratic systems with center and their perturbations," *J. Differential Equations* **109**, 223–273.

Żołądek, H. [1994] "The classification of reversible cubic systems with center," *Topol. Methods Nonlinear Anal.* **4**, 79–136.

Żołądek, H. [1996] "Remarks on: "The classification of reversible cubic systems with center", [Topol. Methods Nonlinear Anal. 4 (1994), 79–136];" *Topol. Methods Nonlinear Anal.* **8**, 335–342.